Study of Site Specific Cleavage of Strongly Bound Hairpin DNAs by Bleomycin

by

Zachary Segerman

A Thesis Presented in Partial Fulfillment
of the Requirements for the Degree
Master of Science

Approved September 2011 by the
Graduate Supervisory Committee:

Sidney Hecht, Chair
Giovanna Ghirlanda
Marcia Levitus

ARIZONA STATE UNIVERSITY

December 2011

ABSTRACT

Natural products that target the DNA of cancer cells have been an important source of knowledge and understanding in the development of anticancer chemotherapeutic agents. Bleomycin (BLM) exemplifies this class of DNA damaging agent. The ability of BLM to chelate metal ions and effect oxidative damage of the deoxyribose sugar moiety of DNA has been studied extensively for four decades.

Here, the study of BLM A_5 was conducted using a previously isolated library of hairpin DNAs found to bind strongly to metal free BLM. The ability of BLM to effect single-stranded was then extensively characterized on both the 3′ and 5′-arms of the hairpin DNAs. The strongly bound DNAs were found to be efficient substrates for Fe·BLM A_5–mediated cleavage. Surprisingly, the most prevalent site of damage by BLM was found to be a 5′-AT-3′ dinucleotide sequence. This dinucleotide sequence and others generally not cleaved by BLM when examined using arbitrarily chosen DNA substrate were found in examining the library of ten hairpin DNAs. In total, 111 sites of DNA damage were found to be produced by exposure of the hairpin DNA library to Fe·BLM A_5.

Also, an assay was developed with which to test the propensity of the hairpin DNAs to undergo double stranded DNA damage. Adapting methods previously described by the Povirk laboratory, one hairpin was characterized using this method. The results were in accordance with those previously reported.

DEDICATION

To my Grandpa Stan

ACKNOWLEDGEMENTS

First, I would like to express my sincere appreciation to my advisor Dr. Sidney Hecht, who has guided my scientific career for four years of study. Without him, my research and this thesis would not have been possible. I would also like to express gratitude to my committee members Dr .Giovanna Ghirlanda and Dr. Marcia Levitus. Their participation in this project was invaluable.

My lab-mates, Dr. Paul Zaleski, Rachel Giroux, Dr. Shengxi Chen and Basab Roy also played a great role in shaping this project, through training, advice and friendship.

I also appreciate the love and support of my family and friends. They gave me the wherewithal to complete this, and without their motivating support none of this would be possible.

Last, but certainly not least, I want to acknowledge Rebecca who has made a great positive difference in my life.

TABLE OF CONTENTS

Page

LIST OF TABLES

LIST OF FIGURES

Figure Page

ABBREVIATIONS

ATP	adenosine triphosphate
aq	aqueous
BLM	bleomycin
°C	degrees celsius
Ci	curie
cpm	counts per minute
dATP	deoxyadenosine triphosphate
dNTP	deoxynucleoside triphosphate
DTT	dithiothreitol
EDTA	ethylenediaminetetraacetic acid
h	hour
mCi	millicurie
mg	milligram
min	minute
mL	milliliter
mmol	millimole
mM	millimolar
µL	microliter
µM	micromolar
ng	nanogram
nm	nanometer
nmol	nmole
nt	nucleotide
pmol	picomole
Pu	purine
Py	pyrimidine
s	second
TBq	terabecquerel
Tris	tris(hydroxymethyl)aminomethane
V	volts
W	watts

Chapter 1

AN OVERVIEW OF DNA AND BLEOMYCIN STUDIES

DNA and Cleavage Reactions

Friederich Miescher discovered deoxyribonucleic acid (DNA) by chance in 1869 while trying to identify the chemical constituents of cells. While studying the pus from used surgical dressings, he isolated a substance he called nuclein from the cellular nucleus which precipitated in acid, and was re-dissolved upon treatment with alkali.[1]

Later study of DNA found that it is composed of repeating nucleotide units. A nucleotide of the DNA is composed of four different nucleobases: adenine (A), thymine (T), guanine (G) and cytosine (C). The nucleobases are covalently linked to a 2-deoxyribose sugar which has a pentavalent phosphate attached to it in the 5′-position. The phosphate provides the linkage through which multiple nucleotides are attached in repetitive strands.[2] The polynucleotide can form a double stranded structure through G:C and A:T base pairs (Figure 1.1). Notably, Watson and Crick determined that these polynucleotides adopted a double helical conformation (Figures 1.1 and 1.2). [3]

The double helix is formed by the binding of two DNA strands in an antiparallel fashion through a cooperative mechanism of π-π helical stacking and hydrogen bonding at the Watson and Crick faces of the DNA nucleobases (Figure 1.1).[2] The sugar and phosphate backbone imparts its own structural features onto the DNA helix, including the presence of two distinct grooves, termed minor and the major (Figure 1.2).[4] In what is thought to be the most biologically prevalent

form of DNA, B-form, the DNA has a narrow minor groove and wide a major groove (Figure 1.3).[4]

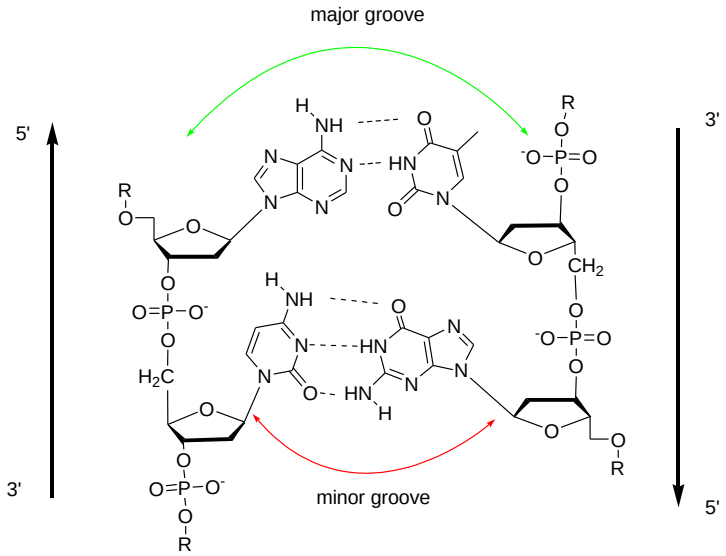

Figure 1.1: Base pair connections made at the Watson-Crick faces of the nucleobases, showing the relative orientation of sugars to each other in an antiparallel fashion. Also indicated is the way in which the glycosidic linkage between ribose and the nucleobase frames the minor and major grooves.

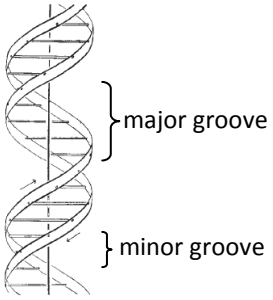

Figure 1.2: A purely diagrammatic image of the DNA double helix from Watson and Crick's classic 1953 publication. The ribbons represent the sugar-phosphate back bone, while the bars represent the hydrogen bonding of the Watson-Crick faces of the AT and GC basepairs. The center line marks the helical axis.[3]

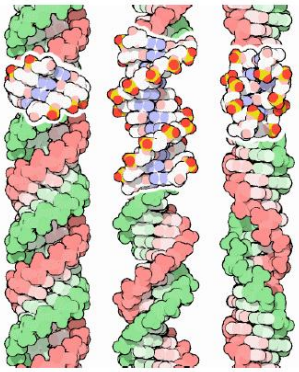

Figure 1.3: The different local structures adopted by the DNA double helix, from left to right: A-DNA, B-DNA and Z-DNA.[2]

DNA functions as the template for the transmission of genetic information.[5] The development and study of drugs that target the DNA of cancer cells are of great interest as chemotherapeutic agents. Historically, some of the first anticancer chemotherapeutic agents were DNA damaging compounds. These classes of damage include alkylation, mediated by agents such a dimethyl sulfate, or cross-linking mustard compounds such as mechlorethamine.[6] These agents damage strands by making the nucleobase itself sucesptible to hydrolysis (dimethyl sulfate) or providing additional strain on the DNA molecule through interstrand cross links. The attachment distorts the structure and allows cleavage of the double-helix (mechlorethamine).[6] The compound studied in this work comprises part of another class of compounds which damage DNA. The family of glycopeptide antibiotics, the bleomycins, effect oxidative damage to the sugar of DNA (Figure 1.4).

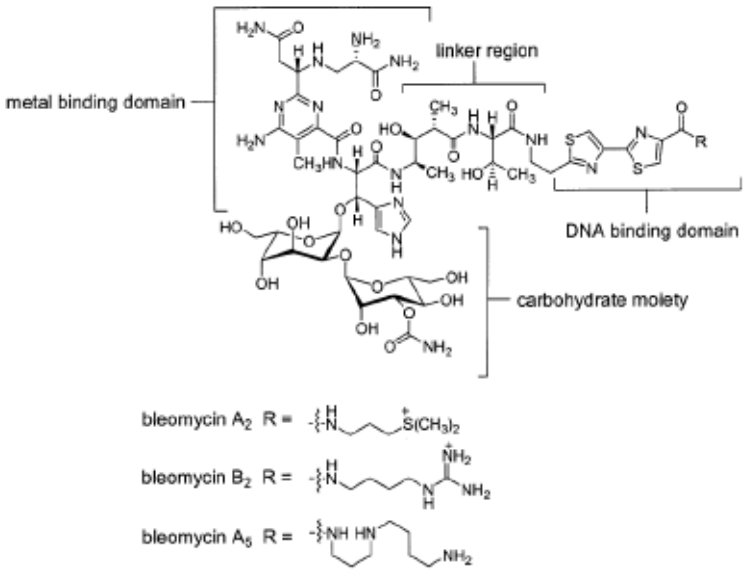

Figure 1.4: The general structure of the family of BLMs, including its structural domains. The R groups below represent differing C-terminal substituents that are the main difference among BLM congeners. [7]

Bleomycin Overview

The BLMs were first isolated from a fungal broth in 1966 by Umezawa and coworkers as copper chelates.[8] BLM has realized success in the treatment of testicular cancer[9] and is an important part of combination therapy for non-Hodgkin's Lymphoma[10] under the commercial name Blenoxane (Bristol-Myers Squib Company). Blenoxane is a mixture of BLM congeners, mainly composed of BLM A_2 and B_2 (Figure 1.4). The cytotoxicity of the drug is attributed to the ability of BLM to bind and degrade DNA in a sequence selective fashion at 5′-GC-3′ and 5′-GT-3′ dinucleotide sequences.[11] BLM also has the ability to bind and degrade RNA in a shape selective fashion.[12] BLM can damage the DNA in

both single-stranded[11,13,14] and double-stranded manners.[15] The latter damage is thought to be the most deleterious to cells as it is more difficult to repair.[16]

BLM requires a metal ion cofactor and oxygen to damage DNA. Analysis of the degradation products of DNA damage indicate that this damage is initiated by abstraction of the C-4′ H in the minor groove of the DNA (Figure 1.1).[17] The ability of BLM to selectively bind and initiate DNA cleavage is due to the complex structure of the molecule. Four domains of BLM can be distinguished: the metal binding domain, the linker region, the DNA binding domain and the carbohydrate moiety (Figure 1.4).[18]

Structural Domains of Bleomycin

The metal binding region contains the nitrogen atoms responsible for chelating a metal ion and activating molecular oxygen, which ultimately leads to DNA cleavage.[19] According to X-ray crystallography of HOO·Co(III)·BLM A_2, the secondary and primary amines of the β-aminoalanine moiety participate in Co(III) coordination, along with the N-1 atom of the β-hydroxyhistidine, the N-5 nitrogen as well as the amide nitrogen of the pyrimidinylpropionamide moiety also coordinate Co(III)·OOH (Figures 1.5 and 1.6).[20] The ability of BLM to chelate metal ions, including Fe, and perform oxidative transformations on DNA and other small molecules draw analogies between it and enzymes such as cytochrome P450, which also chelates iron atoms to oxidize small molecules.[21-23]

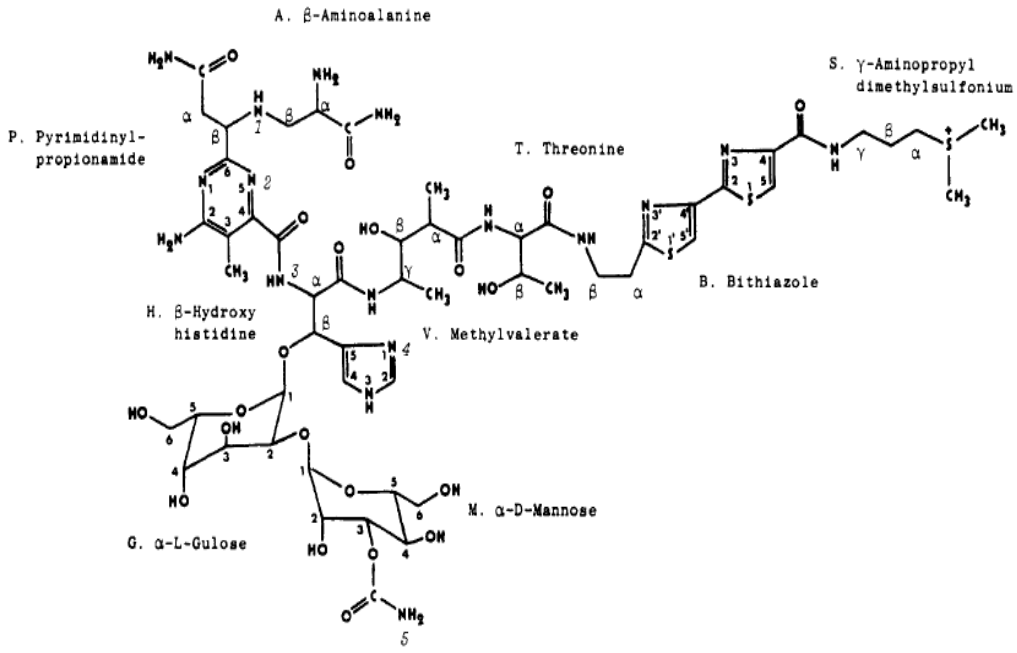

Figure 1.5: A drawing of BLM A_2 with structural features of the compound annotated.[24]

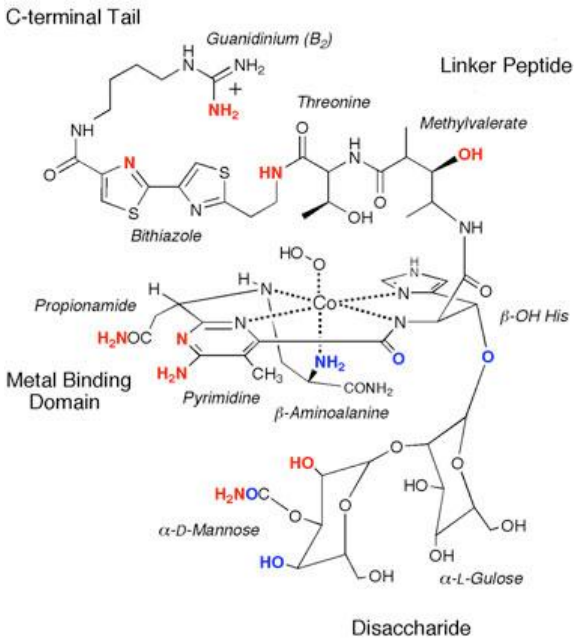

Figure 1.6: The crystal structure of HOO·Co(III)·BLM B_2, detailing the ligand nitrogens.[20]

The pyrimidoblamic acid moiety of this region is also proposed to contribute importantly to DNA binding and strand selectivity. Sequence selectivity is thought to be due to the coordination of the N-1 nitrogen and the C-2 amino groups of the pyrimidoblamic acid to the C-2 amino and N-3 atom of the guanosine 5′ to the Py of the 5′-GPy-3′ cleavage site (Figure 1.7).[16] Alterations of the pyrimidoblamic acid moiety of BLM gave congeners with differing sequence selectivity.[25] Epibleomycin, for example, contains a different stereocenter at the carbon of the β-aminoalanine group marked with an asterisk in Figure 1.7. The epibleomycin congener shows a significant increase in preference for 5′-TG-3′ site selection, a reverse of the 5′-PuPy-3′ selection rule to 5′-PyPu-3′.[25,26] The Hecht laboratory noted that the strand selectivity is also enforced through this geometric conformation suitable to cleavage of only one dinucloetide. For example, the complementary sequence of a 5′-GC-3′ is 5′-GC-3′. Strand selectivity dictates that each site requires a separate binding conformation for cleavage to take place.[27]

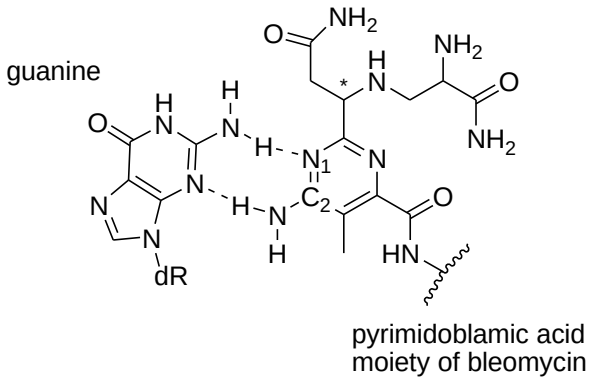

Figure 1.7: Hydrogen bond contacts the pyrimidoblamic acid moiety makes with the floor of the minor groove to enable strand selective cleavage. Adapted from Chen and Stubbe.[16]

The DNA binding domain enhances the ability of the molecule to bind to DNA (Figure 1.4). It contains the bithiazole and C-terminal substituent. There is evidence that the bithiazole moiety can interact with DNA via minor groove binding[28,29] or through intercalation.[30] The C-terminal substituent varies depending upon the specific BLM congener. Displayed in Figure 1.4, the positive charge on the C-substitutent is either permanent (BLM A_2) or the prevalent species at physiological pH (BLM B_2, BLM A_5). The cationic substituent may enhance interaction with the negatively charged DNA phosphate backbone. Removal of the C-terminal substituent diminishes DNA cleavage efficiency tenfold.[31,32]

The linker region is thought to organize the molecule into a compact structure that facilitates DNA cleavage. It is composed of L-threonine and methylvalerate amino acids. Studies detailing the systematic modification of this region have shown that alterations can dramatically alter the DNA cleavage efficiency and ratio of double-stranded DNA damage by BLM. [18,31,33,34] Boger and colleagues found that as long as modifications of this region did not abolish cleavage activity the sequence selectivity was not altered. The ratio of double-stranded to single-stranded damage was affected, however. The presence of L-threoine was strongly preferred over other amino acid analogues.[35]

The carbohydrate moiety of BLM is the disaccharide 2′-O-mannopyranosyl-α-L-gulose modified at the 3′-oxygen of the gulose with a carbamoyl group. The precise function of the disaccharride is still debated. The BLM aglycone functions in a similar manner to the glycosylated BLM (Figure

1.8), however the ratio of single-stranded to double-stranded cleavage is twofold higher for glycosylated BLM. [36,37] The sugar attachment also influences DNA recognition[38], may aid in metal binding[39,40] and may facilitate cellular uptake.[41] DNA and RNA cleavage studies have shown that the α-L-gulose is the sugar most responsible for cleavage potency. Removal of the gulose yielded a BLM analogue that was 2-5 times less efficient at cleaving DNA than BLM A_2. The DNA cleavage efficiency was essentially equivalent to the BLM aglycone, deglycoBLM (Figure 1.8).[36,42]

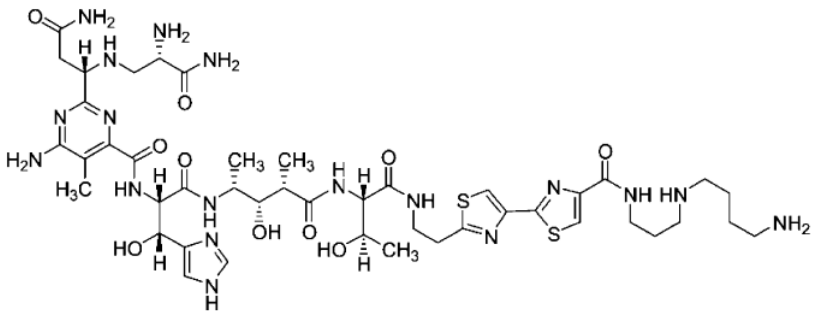

Figure 1.8: The structure of deglycoBLM A_5.[7]

DNA Cleavage by Bleomycin

As explained above, the intricate structure of BLM allows it bind a metal ion, oxygen and DNA, facilitating the abstraction of the 4′-hydrogen atom from the deoxyribose sugar of DNA. BLM, Fe^{2+} and oxygen combine to form a ferric superoxide complex: $^{\bullet}O_2^{-}\cdot$Fe(III)·BLM (Figure 1.9).[43] The superoxide complex gains a proton and an electron to form a HOO·Fe(III) ·BLM, defined as activated BLM, which is the last intermediate detected prior to DNA strand scission.[44,45] Decker et al. recently proposed using experimental and computational analysis

that HOO•Fe(III) •BLM is responsible for abstraction of the C-4′ hydrogen atom, initiating DNA damage.[45]

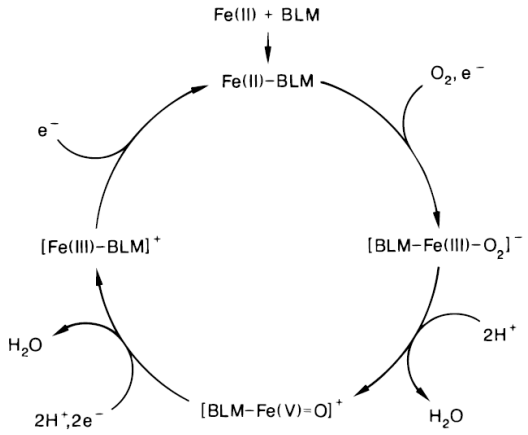

Figure 1.9: Proposed catalytic cycle of Fe·BLM.[18]

Fe·BLM can effect DNA damage through two different pathways. One pathway produces frank strand scission[46] and the other produces an alkali labile lesion.[47] The preferred sequence selectivity, 5′-GPy-3′, results in oxidative damage of the pyrimidine sugar moiety resulting in the release of a base propenal and leaves a phosphoglycolate moiety attached to the 3′-hydroxyl group that is 5′ to the site of damage. The site to the 3′-side of the released base has a 5′-phosphate (Figure 1.10). After activated BLM acts upon the DNA, O_2 can be attached to the sugar creating a 4′-hydroperoxydeoxyribose which undergoes a Criegee-type rearrangement. The resultant six-member heterocycle further rearranges, breaking down to produce a base propenal and a 3′-phosphoglycolate

moiety. An alternate pathway can also occur which does not consume an equivalent of oxygen (Figure 1.11).

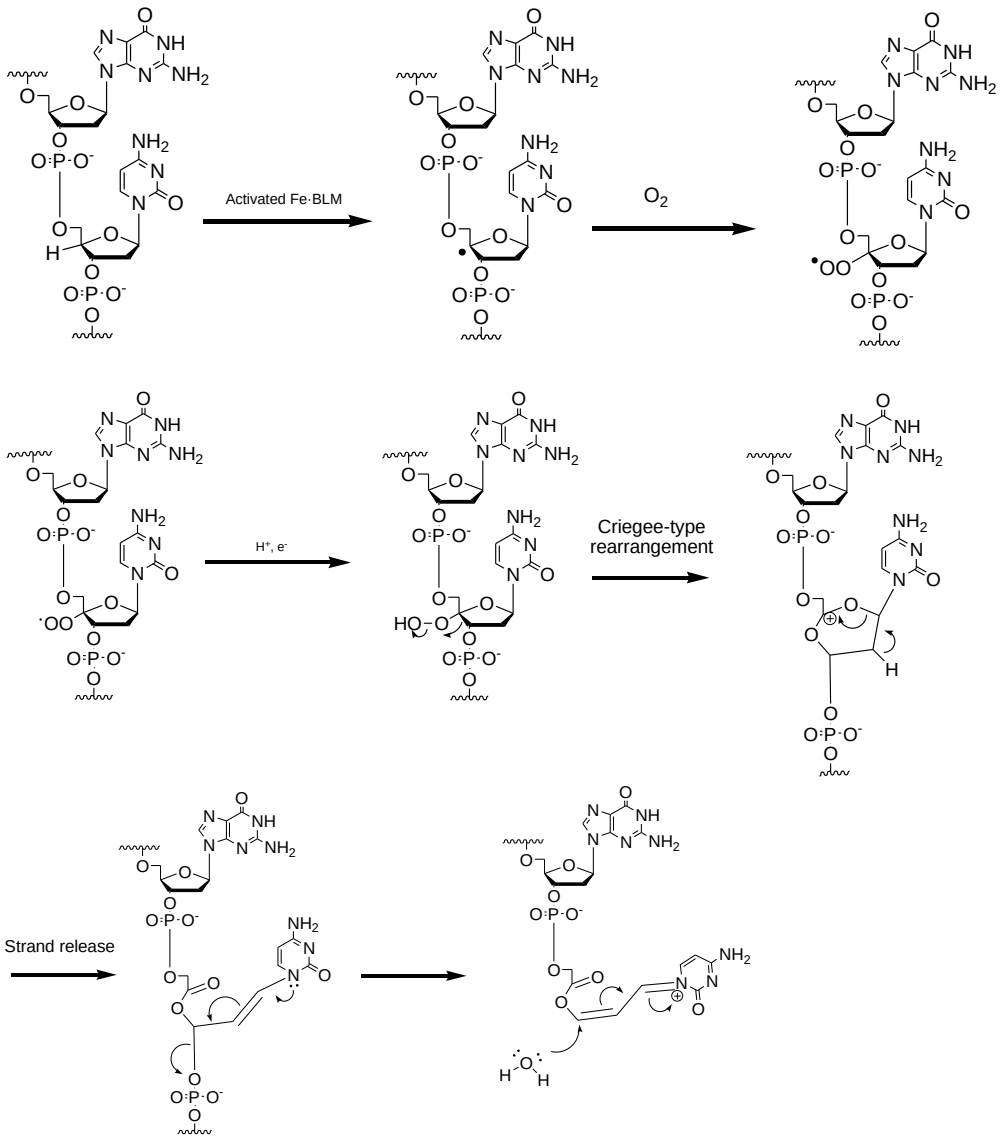

Figure 1.10: A proposed mechanism for the oxygen dependent frank strand scission pathway that accounts for ^{18}O labeling results.[48]

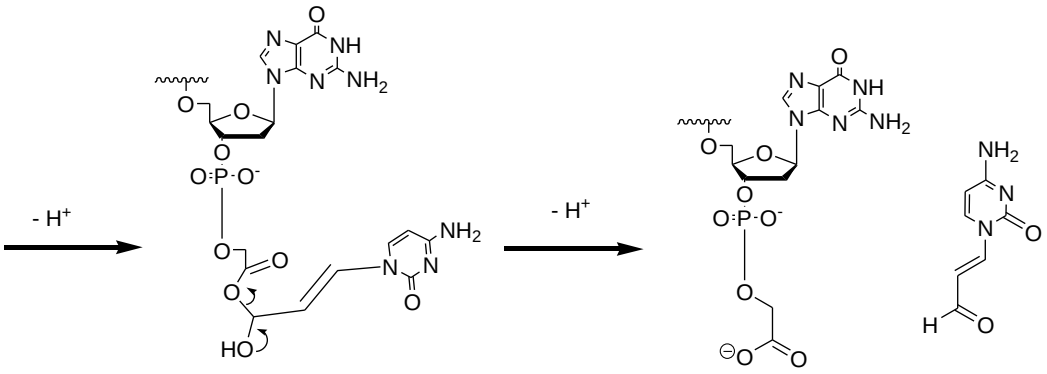

Figure 1.10 cont'd: A mechanism for the frank strand scission pathway which accounts for the incorporation ^{18}O into the ribose sugar structure.[48]

Figure 1.11 presents a mechanism for the production of an alkali labile lesion, starting from the sugar C-4′-radical. This pathway does not require the incorporation of O_2 to the sugar radical. After oxidation to the C-4′-radical water is incorporated into the five-membered ring of ribose. Rearrangement effects base release and a 4′-ketoaldehyde remains attached to the DNA strand. The 4′-ketoaldehyde is in equilibrium with a 4′-hydroxyabasic site, the latter of which likely predominates in nature (Figure 1.11).[49] Upon treatment with alkali this lesion rearranges to 2-hydroxycyclopentenone.[49]

One molecule of BLM can effect cleavage upon a DNA molecule twice, resulting in double-stranded (ds)DNA damage.[51] Double-stranded DNA damage is thought to be responsible for the antitumor activity associated with BLM treatment. Povirk and colleagues reported sequence selection rules for BLM induced dsDNA damage based on the observed cleavage sites of a restriction fragment.[52] The first site of damage is generally a site preferred by BLM for damage (5′-GPy-3′) and the second site of cleavage is either straight across from

the initial site, or staggered in the 5′ direction on the opposing strand. The C-4′ hydrogen of the second site of damage is oriented in the opposite direction, requiring that BLM undergo significant reorganization of binding to cleave at the second site. For a 5′-GPyPy-3′ the second site of damage was usually directly opposite to the initial site of cleavage. If the site was 5′-GPyPu-3′, damage generally occurred directly opposite to the Pu site. This results in a fragment staggered by one base in the 5′ direction (Figure 1.12). Povirk and coworkers postulated that the primary site of damage must undergo the frank strand scission pathway in order for activated BLM to be regenerated to cleave the DNA again (Figure 1.10). The secondary site can follow either the oxygen dependent or independent cleavage pathway. The activated BLM must also reorganize dramatically in order to produce cleavage at the 4′ hydrogen on the opposing strand.[53] At present there is no direct experimental evidence that supports this suggestion.

In order for two oxidation events to take place near each other spatially and temporally a remarkable reactivation and reorganization of DNA–BLM binding must occur without dissociation. Indirectly, $HOO{\cdot}Co^{III}{\cdot}$BLM was observed via 2D-NMR study to bind in an intercalative mode via the bithiazole moiety, rotate about the axis of the bithiazole 180^{o} and rotate 117^{o} perpendicular to the helical axis of DNA.[54-56] Fe·BLM was proposed to oxidize at the primary site and then access the other site of cleavage through this remarkable ring-flip mechanism (Figure 1.13).[57]

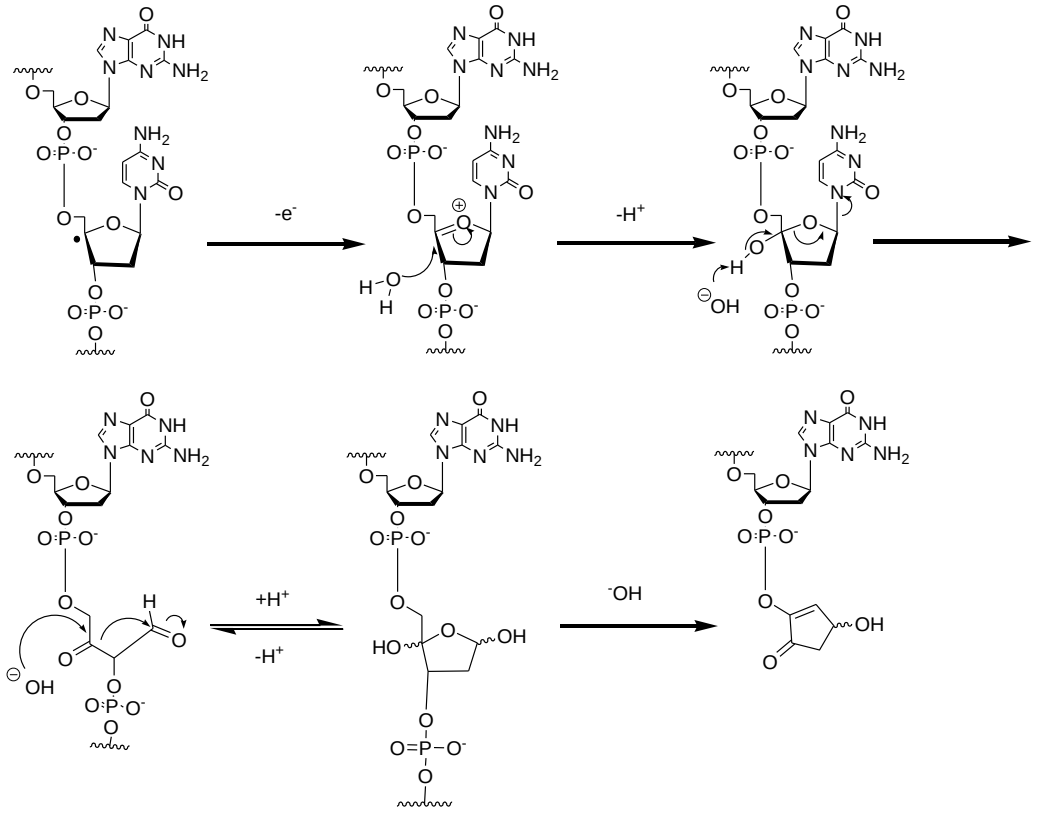

Figure 1.11: A mechanism for the production of 4′-hydroxyabasic acid. Upon treatment with alkali the strand is released and the structure of the sugar 3′ to the site of damage collapses to a 2-hydroxycyclopentenone.[49,50]

Figure 1.12: The cleavage patterns produced by double-stranded DNA damage with BLM observed by Povirk et al.[52]

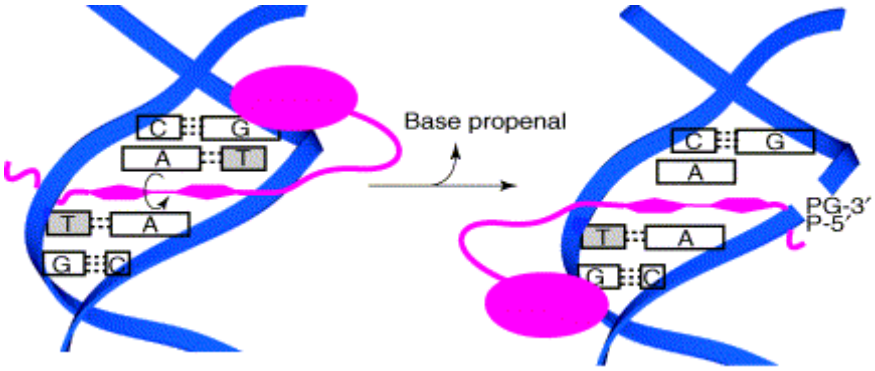

Figure 1.13: Stubbe model of BLM mediated double-strand DNA cleavage.[57]

The Hecht laboratory has also studied another mode of dsDNA cleavage that does not require reorganization of BLM. Keck et al. observed double-stranded cleavage of the Drew-Dickerson dodecamer more apposite of a minor groove binding agent, effecting cleavage with a 3-nt 3′ overhang,[58] as opposed to the 5′ overhangs and blunt–ended fragments reported by the Povirk laboratory.[52] The Hecht laboratory documented 43% double-stranded cleavage.[58] The 2D-NMR study of the Zn·BLM–DNA complex indicated a complex where DNA offered both C4′-H atoms in close spatial proxmitiy to the Fe^{2+} in the metal binding domain.[58]

The 2001 study of the Drew-Dickerson dodecamer with BLM A_2 was a foundational work in the study of BLM–DNA binding.[58] The Hecht laboratory was the first to report and suggest a model where the global structure of DNA could be recognized by BLM and offer sites of cleavage that did not accord to the 5′-GPy-3′ sequence selection (Figure 1.13).[58] More recent studies by Hecht and colleagues on hairpin DNAs selected for their ability to bind BLM tightly have shown that the relationship between DNA binding and DNA cleavage is more

complex a relationship than previously believed.[7,59,60] Chapter 2 discusses the previous studies in some detail. It also describes current progress made in the present work towards the study of DNA binding and DNA cleavage with strongly bound DNAs as substrates for damage.

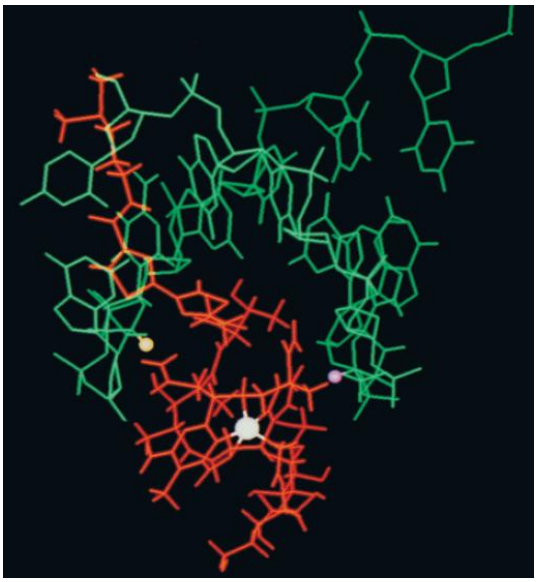

Figure 1.14: A stereoview looking into the minor groove of the Drew-Dickerson dodecamer complexed with BLM A_2. The yellow and purple balls represent C4′-H atoms, while the white ball represents the metal center of BLM. This image indicates that the 3-nt separation places both hydrogens in proximity to the metal center of BLM. This facilitates dsDNA cleavage by the drug without reorganization.[58]

Chapter 2

CLEAVAGE SITE ANALYSIS OF STRONGLY BOUND DNA HAIRPINS REACTED WITH BLEOMYCIN A_5

Introduction

The ability of BLM to bind to DNA and the ability to degrade DNA in a sequence selective fashion have been examined extensively, but independently of one another. Studies concerned with DNA damage activity focus on the end products of DNA cleavage. The studies concerned with DNA–binding focus on metalloBLMs such as Co[61,62] and Zn.[28,63] The relationship of these metalloBLMs to Fe·BLM is ambiguous, however. With few exceptions the studies also do not test the relationship between binding and cleavage directly. One study that did test the relationship directly employed Co.[64] The applicability of the study of this metalloBLM to clinical use of the drug is not certain.

The experimental conditions employed in these cleavage studies also present potential limitations in the application of the findings to the action of BLM in a clinical setting. These conditions include the high stoichiometric ratio of BLM to DNA and arbitrarily chosen DNA substrates. In clinical use, the effective dose of BLM is very low, *ca*. 5 μmol, and possible DNA targets are in vast excess.[60] Given this ratio, one could assume that the obligatory binding step preceding cleavage is very selective, and few sequences are selected by BLM for potential cleavage. These selected sequences could be quite different from what has been learned from studies using arbitrarily chosen DNA sequences and high molar ratios of BLM to DNA.

Recently, the Hecht laboratory reported a study relating BLM binding directly to cleavage with Fe·BLM, which is believed to be the therapeutically relevant species (Figure 2.1).[59] Briefly, strongly bound sequences were identified through the first step of a SELEX-type procedure. A mobile phase containing a library of 64-mer hairpin DNA sequences with an 8-nucleotide (nt) randomized region was passed over a stationary phase of resin-bound BLM A_5. The strongly bound DNAs were collected and then were sequenced (Table 2.1). The Hecht laboratory then quantified the binding efficiencies of these DNAs using a competition assay employing a profluorescent nucleotide as a reporter molecule.[60,65]

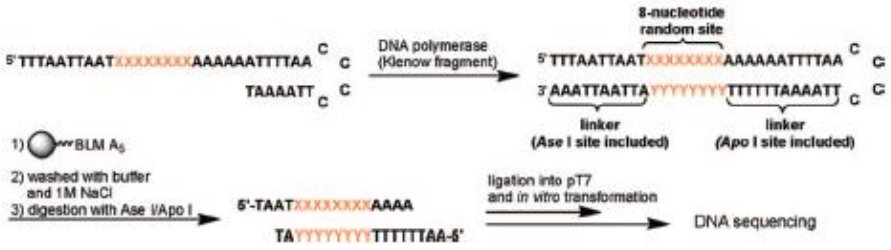

Figure 2.1: A scheme for generating a library of DNAs to expose to resin bound BLM A_5 in order to capture DNAs that are strongly bound.[60,65]

The competition assay involves a 16-nt hairpin DNA that contains a high efficiency cleavage site with a modified profluorescent DNA nucleobase at this preferred cleavage site (Figure 2.2). This substrate is cleaved stoichiometrically by Fe·BLM.[65] Upon release of this base or base propenal by the action of Fe·BLM, fluorescence can be measured. The suppression of fluorescence upon addition of the 64-nt hairpin to the mixture would then quantitatively reflect the

binding preference of BLM for the 64-nt hairpin DNA, given a choice between the two substrates. Hecht and coworkers reported that when used in amounts equivalent to the 16-nt hairpin DNA substrate and Fe·BLM, the ten DNA hairpins suppressed cleavage of the 16-nt modified hairpin by between 76 and 97% (Table 2.2).[60] In addition, Hecht laboratory performed an initial examination of the relationship between DNA binding and DNA damage through cleavage site analysis using 5′-^{32}P end labeled 64-nt hairpin DNAs and high resolution polyacrylamide gel electrophoresis.

Table 2.1: The 64-nt hairpin DNAs isolated by Hecht and coworkers after the first step of SELEX-procedure.[60]

	5′TTTAATTAATXXXXXXXXAAAAAATTTTAA 3′AAATTAATTAXXXXXXXXTTTTTTAAAATT		C C C C
DNA 1	5′AGATCATG 3′TCTAGTAC	DNA 2	5′CGTGACGC 3′GCACTGCG
DNA 3	5′TAAGTGGG 3′ATTCACCC	DNA 4	5′GAGAGGAT 3′CTCTCCTA
DNA 5	5′ACAGAATA 3′TGTCTTAT	DNA 6	5′CTACTAAA 3′GATGATTT
DNA 7	5′TACGCGCA 3′ATGCGCGT	DNA 8	5′GGGTACCT 3′CCCATGGA
DNA 9	5′CGTTGTTA 3′GCAACAAT	DNA 10	5′CGCCATTG 3′GCGGTAAC

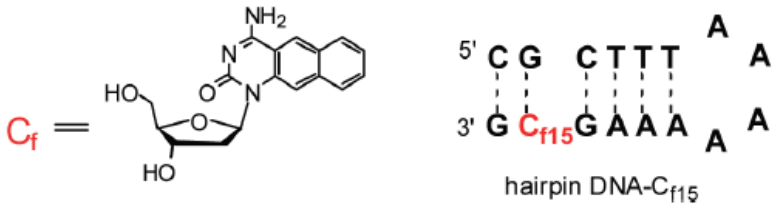

Figure 2.2: Chemical structure of a 16-nt hairpin DNA-C_{f15} having the 2′-deoxyriboside of 4 aminobenzo[*g*]quinazoline-2-one (C_f) at position 15.[65]

Table 2.2: The binding specificity of the hairpin DNAs as recorded from the suppression of cleavage by Fe·BLM A_5 of a 16-nt with a profluorescent nucleotide.[60,65]

hairpin DNA	binding specificity (%)	hairpin DNA	binding specificity (%)
1	82	**6**	81
2	97	**7**	97
3	76	**8**	92
4	79	**9**	89
5	90	**10**	86

The study revealed a complex relationship between binding and cleavage. Many of the DNAs that are bound strongly present at least one 5′-GT-3′ or 5′-GC-3′ dinucleotide sequence (Table 2.1). These sequences also appear as the dominant sites of damage in the high resolution polyacrylamide electrophoresis experiments.[60] Other hairpins are not as strongly bound and offer no canonical dinucleotide sequences, but are still cleaved avidly by BLM. The wide range of sequence motifs and cleavage efficiencies identified in this study indicate a much more complex picture of BLM–DNA binding and cleavage than initially

presumed from studies employing arbitrary DNA sequences with BLM in stoichiometric excess.

The analysis of these hairpin DNAs was continued with another study by Giroux and Hecht detailing the interaction and chemistry of the hairpin DNAs with BLM A_5 and deglycoBLM A_5 (Figure 1.8).[7] This study showed that deglycoBLM A_5 cleaved the hairpins in a manner similar to BLM A_5, although in diminished potency. Interestingly, deglycoBLM A_5 produced DNA damage on the hairpin DNAs that appeared only in the oxygen independent pathway, whereas BLM A_5 did not.[7] The present work builds on this study, providing a comprehensive picture of DNA cleavage by Fe·BLM A_5 by using both 5′ and 3′-^{32}P end labeling to fully characterize all sites of cleavage inflicted on these specially selected hairpin DNAs by BLM A_5.

This work then further characterizes the DNAs for their propensity to be cleaved twice by one molecule of BLM (double-stranded cleavage). Adapting methodologies from the Hecht[58] and Povirk[52] laboratories to examine the hairpin DNAs, an assay was developed for the initial examination of double-stranded (ds)DNA damage. Application of this method to the current library of 10 hairpin DNAs would then provide insights into the relationship between binding and dsDNA damage. Plausibly, the effectiveness of BLM is due to its ability to identify specific sequences for cleavage and damage both DNA strands in a single process, thereby explaining its exceptional antitumor potency.

Results

The recently reported library of hairpin DNAs, of the form 5′-TTTAATTAATXXXXXXXXAAAAAATTTTAACCCCTTAAAATTTTTTYYYYYYYYYATTAATTAAA-3′, were characterized by high resolution polyacrylamide electrophoresis and the cleavage suppression of a previously studied 16-nt hairpin with a pro-fluorescent hairpin DNA.[60] The hairpin DNAs were collected via the first step of a SELEX-type procedure to provide hairpin DNA sequences that are strongly bound by metal free BLM A_5. These hairpin DNAs were found to inhibit cleavage from 76% to 97%. The following results describe analysis of cleavage of the 10 hairpin DNAs by denaturing polyacrylamide gel electrophoresis using 5′ and 3′-^{32}P end labeling, allowing for the analysis of every site cleaved by Fe(II)·BLM A_5 in the hairpin DNA library.

DNA **1** was treated with increasing concentrations Fe(II)·BLM A_5 and several strong cleavage sites were observed in both 5′ and 3′-^{32}P end labeling. Figure 2.3A[60] (gel performed by Dr. Qian Ma) clearly shows the presence of six cleavage sites. None of these sites follow the canonical dinucleotide cleavage sites for BLM A_5. These sites include A_9, T_{10} A_{13}, T_{14} , and A_{19}. There are several unusual sites and sequence motifs worthy of note, namely the 5′-PuPu-3′ cleavage sites at 5′-GA_9-3′, 5′-GA_{13}-3′ and 5′-GA_{19}-3′. The other nucleobase cleaved on this hairpin, thymidine, follows the more classic motif of 5′-PuPy-3′. The purine was not the usual guanosine, but adenine. These dinucleotide sequences were 5′-AT_{10}-3′, 5′-AT_{14}-3′ and 5′-AT_{17}-3′.

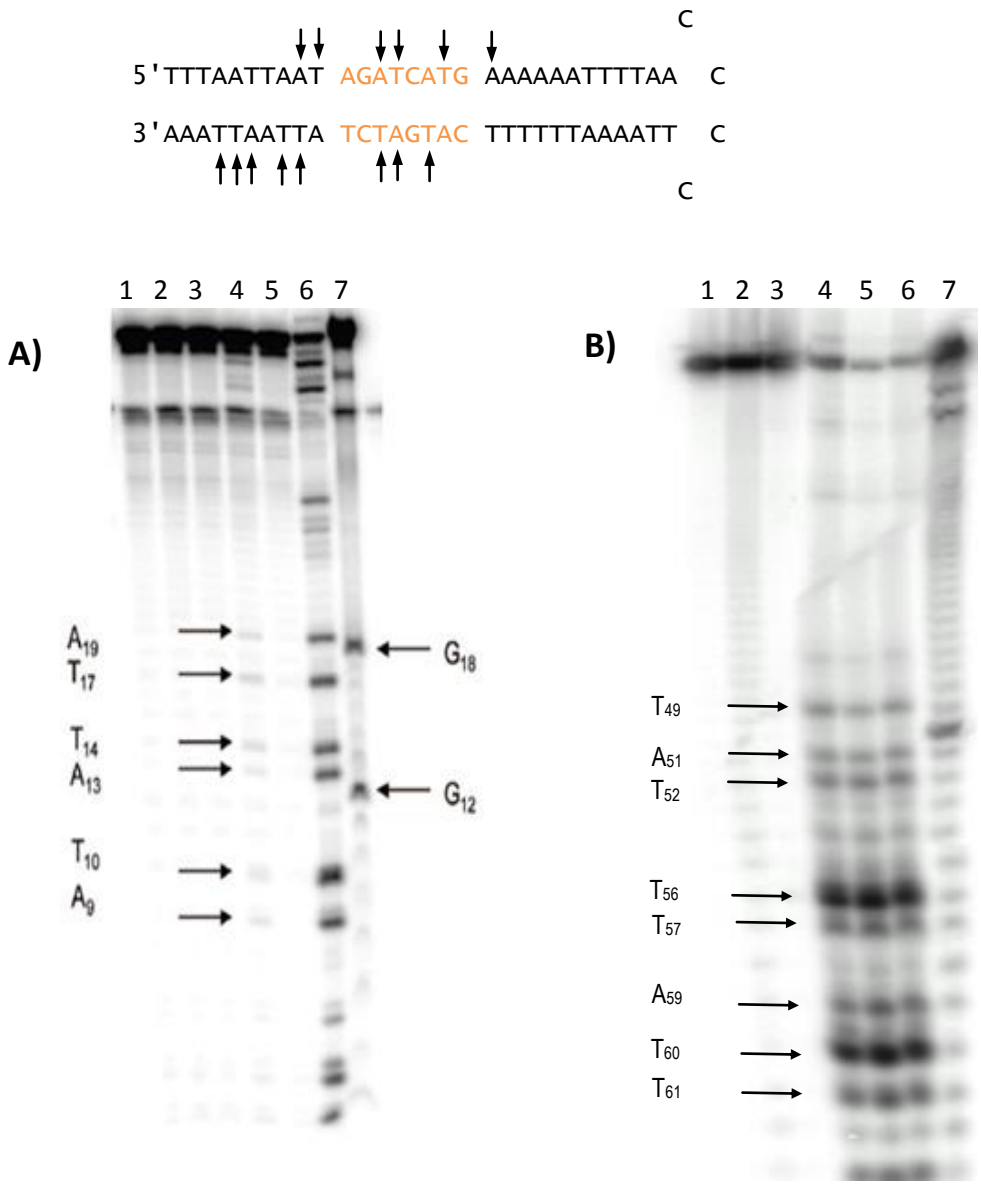

Figure 2.3: A) Sequence-selective cleavage of [5′-^{32}P]-end labeled 64-nt hairpin DNA **1** by BLM A_5. Lane 1, radiolabeled **1** alone; lane 2, 20 μM Fe^{2+}; lane 3, 5 μM BLM A_5; lane 4, 5 μM Fe(II) ·BLM A_5; lane 5, 20 μM BLM A_5; lane 6, 20 μM Fe(II) ·BLM A_5; lane 7, G-lane.[10] B) Sequence-selective cleavage of [3′-^{32}P] end labeled 64-nt hairpin DNA **1** by BLM A_5. Lane 1, radiolabeled **1** alone; lane 2, 10 μM Fe^{2+}; lane 3, 10 μM BLM A_5; lane 4, 1 μM Fe(II) ·BLM A_5; lane 5, 5 μM Fe(II) ·BLM A_5; lane 6, 10 μM Fe(II) ·BLM A_5; lane 7, G-lane.

The 3′-^{32}P end labeling cleavage experiment (Figure 2.3B) of DNA **1** showed very similar results to Figure 2.3A, as the hairpin contained no classically cleaved dinucleotide sequences for Fe(II)·BLM A_5, but did contain several strong sites for cleavage, which were close to the radiolabel. The sites T_{49}, A_{51}, T_{52}, T_{56}, T_{57}, A_{59}, T_{60} and T_{61} were cleaved by BLM A_5 at the 3′-arm of the hairpin DNA. The very strong site at T_{56} is actually within the flanking region of the hairpin DNA. This site is a 5′-AT-3′ site, similar to the sites found on the 5′- arm of the hairpin DNA. However there was also a very unusual 5′-TT-3′ cleavage band, which albeit weak, is generally not reported in the literature that has employed arbitrarily chosen DNA substrates.

DNA **2** differed from DNA **1** at the 5′-arm of the hairpin DNA. DNA **2** contained two traditionally cleaved dinucleotide sequences (5′-GC-3′). Although there was cleavage at these sites, it was cleaved comparatively weakly to the other classic cleavage motif of 5′-GT-3′ which represented the strongest site of cleavage (Figure 2.4A, performed by Dr. Qian Ma).[60] DNA **2** also had a binding efficiency of 97%, which is the highest value recorded in the competition assay. The lesion at A_{15} is a 5′-PuPu-3′ dinucleotide sequence motif. It was cleaved quite weakly in comparison to both the classic cleavage motifs. This 5′-^{32}P end labeled experiment also did not demonstrate the presence of cleavage in the flanking regions as definitively as the 3′-^{32}P end labeled hairpin DNA **1**.

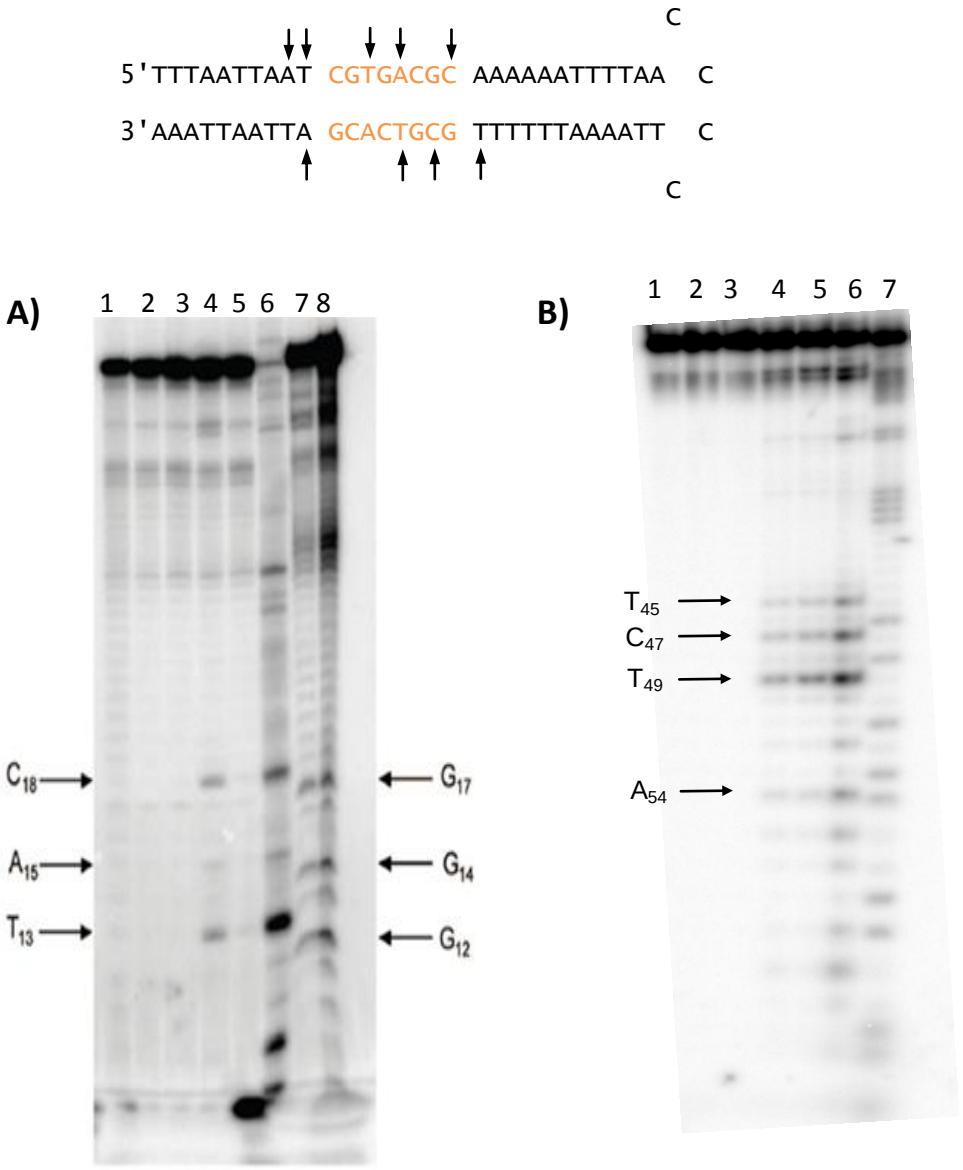

Figure 2.4: A) Sequence-selective cleavage of [5′-^{32}P]-end labeled 64-nt hairpin DNA **2** by BLM A_5. Lane 1, radiolabeled **2** alone; lane 2, 20 μM Fe^{2+}; lane 3, 5 μM BLM A_5; lane 4, 5 μM Fe(II) ·BLM A_5; lane 5, 20 μM BLM A_5; lane 6, 20 μM Fe(II) ·BLM A_5; lane 7, G+A lane; lane 8, G-lane. B) Sequence-selective cleavage of [3′-^{32}P]-end labeled 64-nt hairpin DNA **2** by BLM A_5. Lane 1, radiolabeled **2** alone; lane 2, 10 μM Fe^{2+}; lane 3, 10 μM BLM A_5; lane 4, 1 μM Fe(II) ·BLM A_5; lane 5, 5 μM Fe(II) ·BLM A_5; lane 6, 10 μM Fe(II) ·BLM A_5; lane 7, G+A lane.

The 3′-^{32}P end labeled hairpin DNA **2** contained two classically cleaved dinucleotide sequences. The most preferred of these was 5′-GT_{49}-3′ (Figure 2.4B). These two dinucleotide sequences represented the strongest sites of cleavage. There were two very weak cleavages at T_{45} and A_{54}, including a rarely reported 5′-PyPy-3′ sequence motif. Work by Ma et al. reported the binding specificity of DNA **2** as 97%, which was markedly higher than that of DNA **1** (82%). It is of interest to note that the number of cleavage sites was less on both arms of the hairpin DNA for DNA **2** compared to DNA **1**.

Hairpin DNA **3** provided very interesting cleavage results despite its comparatively low binding specificity reported by the Hecht laboratory in 2009 as 76%.[60] The hairpin sequence contains four G:C base pairs, and only one 5′-GPy-3′ site, which was cleaved, but with an intensity similar to that of the other sites on the 5′-^{32}P end labeled arm (Figure 2.4A, performed by Qian Ma).[60] The 5′-arm was cleaved six times at the sites A_8, A_9, T_{10}, A_{12}, T_{15} and A_{19}. A 5′-PyPu-3′ cleavage site at T_{10} was the strongest relative site of cleavage on this arm of the hairpin DNA. Radiolabeling the 5′-arm provided a comparable number of cleavage sites compared to DNA **1**, with six, while the 3′-arm of hairpin DNA **3** showed a substantially different result.

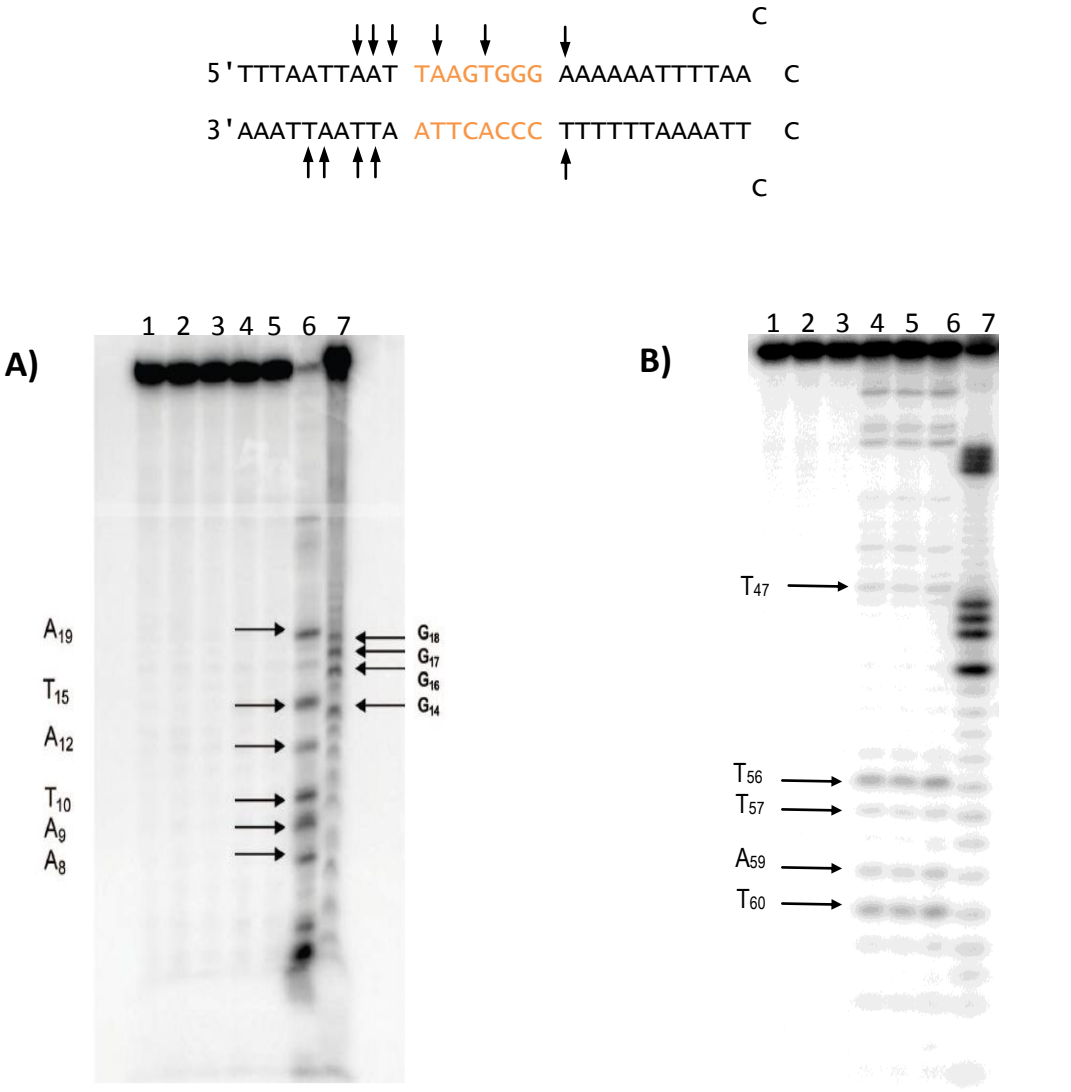

Figure 2.5: A) Sequence-selective cleavage of [5′-^{32}P]-end labeled 64-nt hairpin DNA **3** by BLM A_5. Lane 1, radiolabeled **3** alone; lane 2, 20 μM Fe^{2+}; lane 3, 5 μM BLM A_5; lane 4, 5 μM Fe(II) ·BLM A_5; lane 5, 20 μM BLM A_5; lane 6, 20 μM Fe(II) ·BLM A_5; lane 7, G-lane.[60] B) Sequence-selective cleavage of [3′-^{32}P] end labeled 64-nt hairpin DNA **3** by BLM A_5. Lane 1, radiolabeled **3** alone; lane 2, 10 μM Fe^{2+}; lane 3, 5 μM BLM A_5; lane 4, 1 μM Fe(II) ·BLM A_5; lane 5, 2.5 μM Fe(II) ·BLM A_5; lane 6, 5 μM Fe(II) ·BLM A_5; lane 7, C-lane.

Hairpin DNA **3** was cleaved at T_{46}, T_{56}, T_{57}, A_{59}, and T_{60} when 3′-^{32}P end labeled (Figure 2.5B). The strongest cleavage sites occurred at T_{56} and T_{60}. There were no clear amounts of cleavage within the randomized region, as opposed to the cleavage that appeared on the 5′-^{32}P end labeled hairpin DNA **3**. This preference to cleave the 5′-arm is of special note as hairpin DNA **3** was the only example of the hairpin DNAs tested that demonstrated no clear cleavage in the randomized region when the 3′-arm was ^{32}P-end labeled.

Hairpin DNA **4** (5′-^{32}P end labeled) is shown in Figure 2.6A (polyacrylamide gel performed by Qian Ma).[60] The reported binding specificity of this hairpin DNA was 79%, which is relatively low compared to the other hairpin DNAs. It does not contain any classic sequence motifs for cleavage, but showed a comparatively strong cleavage site at 5′-GA_{12}-3′. The other sites occurred at T_9, T_{10}, A_{14}, A_{17} and T_{18}. These sites are all 5′-PuPy-3′ sequence motifs, excepting A_{17} which is a 5′-PuPu-3′ sequence. Similar to hairpin DNA **3**, there was a divergence in the cleavage that was observed for BLM A_5 on the opposing arm.

The 3′-^{32}P end labeled hairpin DNA **4** showed cleavage at three sites, all of which are thymidines, namely at T_{48}, T_{53} and T_{56} (Figure 2.6B). The 3′-arm showed fewer cleavage sites, but comparatively similar amounts of cleavage. There was no appreciable cleavage in the flanking region. This sequence composition was similar to that offered by hairpin DNA **3** which also showed a similar divergence in the number of cleavage sites on alternate arms of the hairpin DNA, but both hairpin DNAs shared similar binding specificities.

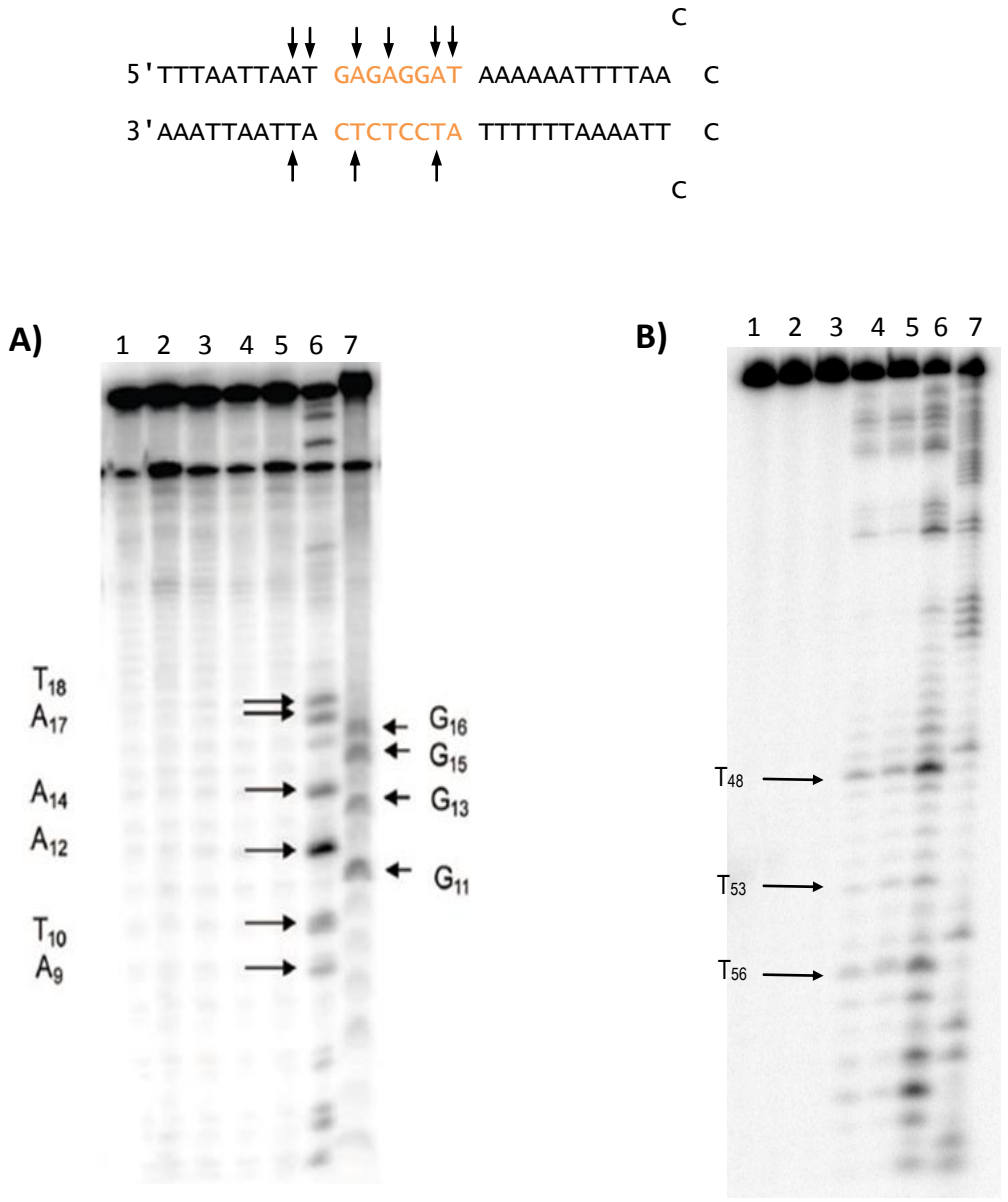

Figure 2.6: A) Sequence-selective cleavage of [5′-^{32}P]-end labeled 64-nt hairpin DNA **4** by BLM A_5. Lane 1, radiolabeled **4** alone; lane 2, 20 μM Fe^{2+}; lane 3, 5 μM BLM A_5; lane 4, 5 μM Fe(II) ·BLM A_5; lane 5, 20 μM BLM A_5; lane 6, 20 μM Fe(II) ·BLM A_5; lane 7, G-lane.[60] B) Sequence-selective cleavage of [3′-^{32}P] end labeled 64-nt hairpin DNA **4** by BLM A_5. Lane 1, radiolabeled **4** alone; lane 2, 10 μM Fe^{2+}; lane 3, 5 μM BLM A_5; lane 4, 1 μM Fe(II) ·BLM A_5; lane 5, 5 μM Fe(II) ·BLM A_5; lane 6, 10 μM Fe(II) ·BLM A_5; lane 7, G+A lane.

BLM A_5 cleaved hairpin DNA **5** at thirteen sites on the 5′-arm. Hairpin DNA **5**, remarkably, contains no 5′-GPy-3′ dinucleotide sequences on its 5′–arm either (Figure 2.7A). DNA **5** was cleaved at the most sites of any hairpin DNA in this library of strongly bound hairpin DNAs, but the binding specificity of 90% was not the highest measured by Ma et al.[60] The sites of cleavage included 5′-TT_7-3′, 5′-TA_9-3′ and 5′-AA_{10}-3′ inside the flanking region, while relatively strong cleavage occurred at 5′-GA_{15}-3′ in the randomized region of the hairpin. The other sites cleaved by BLM A_5 all follow unusual sequence specificities, and the DNA was cleaved many times.

The 3′-arm of the hairpin DNA **5** was cleaved in a very similar manner to the 5′-arm. The 5′-GT_{54}-3′ was the preferred site of cleavage, which was consistent with the expected cleavage pattern for BLM (Figure 2.7B). Thirteen other sites were also cleaved by BLM, albeit relatively weakly. A noteworthy site of unusual cleavage, 5′-TG_{53}-3′, follows the unusual sequence selective pattern of a 5′-PyPu-3′. In summary, hairpin DNA **5** was cleaved avidly by Fe·BLM A_5 within and without the randomized region of the hairpin DNA on both arms.

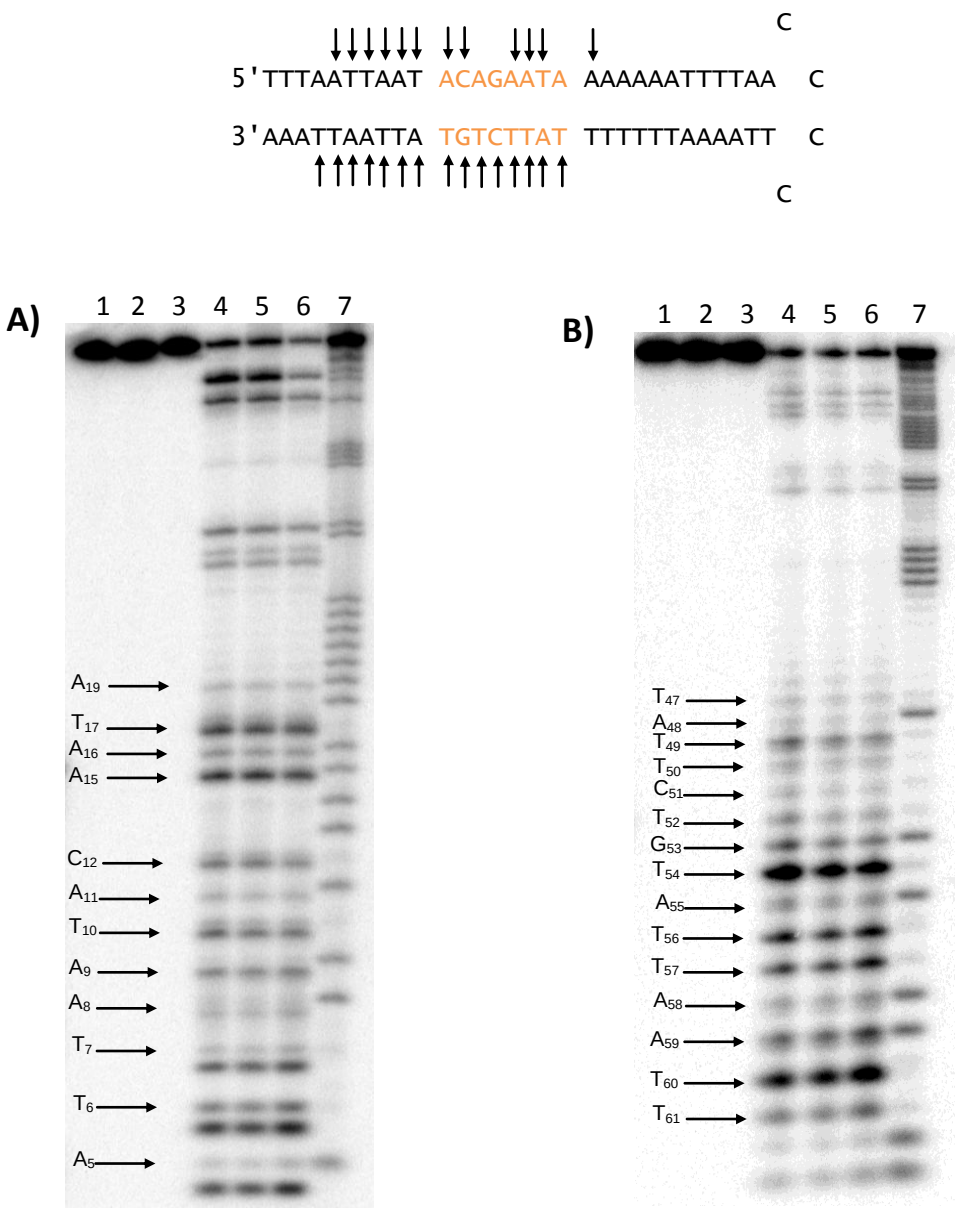

Figure 2.7: A) Sequence-selective cleavage of [5′-^{32}P]-end labeled 64-nt hairpin DNA **5** by BLM A_5. Lane 1, radiolabeled **5** alone; lane 2, 20 μM Fe^{2+}; lane 3, 5 μM BLM A_5; lane 4, 5 μM Fe(II) ·BLM A_5; lane 5, 20 μM BLM A_5; lane 6, 20 μM Fe(II) ·BLM A_5; lane 7, G+A lane. B) Sequence-selective cleavage of [3′-^{32}P]-end labeled 64-nt hairpin DNA **5** by BLM A_5. Lane 1, radiolabeled **5** alone; lane 2, 10 μM Fe^{2+}; lane 3, 5 μM BLM A_5; lane 4, 1 μM Fe(II) ·BLM A_5; lane 5, 5 μM Fe(II) ·BLM A_5; lane 6, 10 μM Fe(II) ·BLM A_5; lane 7, G+A lane.

Hairpin DNA **6** also lacked any dinucleotide sequences commonly cleaved strongly by Fe·BLM. The binding efficiency of this DNA was also lower, 82% (Figure 2.8A). Despite this, DNA **6** still underwent cleavage at seven sites on its 5′-arm, including the unusual 5′-AC_{14}-3′ and 5′-CT_{15}-3′ sites in the randomized region of the hairpin. The flanking region, near the radiolabel was cleaved at more sites than the randomized region. These sites included 5′-AA_5-3′, 5′-AT_6-3′ and 5′-TT_7-3′. The sites A_9 and T_{10} were also cleaved. Interestingly, the 5′-TA_8-3′ was not cleaved on this hairpin DNA.

Figure 2.8B shows the cleavage sites on the 3′-arm of hairpin DNA **6**. There were fewer sites available to BLM on this side of the hairpin DNA, with only one site of cleavage in the randomized region of the hairpin DNA (5′-AT_{52}-3′). The rest of the cleavage occurred in the randomized region at A_{55}, T_{56}, A_{58} and T_{59}. To summarize, this hairpin DNA was cleaved at 12 sites on both arms and each one was a dinucleotide sequence usually not cleaved by BLM A_5. The relative paucity of cleavage on this hairpin DNA compared to DNA **5** is notable, and perhaps can be explained by the lower binding specificity of this DNA.

Sequence selective cleavage of DNA **7** is presented in Figure 2.9. The 5′-arm of hairpin DNA **7** is presented in Figure 2.9A. Hairpin DNA **7** was bound exceptionally well by BLM A_5, with a measured value of 97% in the binding specificity assay, the highest recorded value in the assay. Except for two sites at A_9 and T_{10}, the hairpin **7** was cleaved all within the randomized portion of the DNA. The only nucleotides not cleaved were G_{14} and G_{16}. The hairpin contains two 5′-GC-3′ dinucleotide sequences. The 5′-GC_{17}-3′ dinucleotide sequence was

the preferred site of cleavage on the 5′-arm of hairpin DNA **7.** Remarkably, the 5′-GC_{15}-3′ site was not cleaved to any degree beyond that of the other sites of cleavage.

The 3′-arm of hairpin DNA **7** differed from the 5′-arm in respect to distribution of cleavage sites; most of the cleavage sites occurred in the flanking region of DNA **7** (Figure 2.9B). This preference is interesting to note because of the presence of three 5′-GPy-3′ cleavage motifs in the randomized region. Of the three sites, two were cleaved: 5′-GC_{51}-3′ and 5′-GT_{53}-3′. The lack of cleavage at 5′-GC_{49}-3′ is notable. The 5′-GT_{53}-3′ site was the most efficiently cleaved site on the 3′-arm of this hairpin. To conclude, BLM A_5 cleaved DNA **7** at 15 sites and had the highest binding efficiency measured (97%). Interestingly, BLM A_5 preferred certain 5′-GPy-3′ dinucleotide sites over others, with 5′-GT-3′ being the most efficiently cleaved, and certain other sites (5′-GC_{51}-3′) not undergoing cleavage.

The binding specificity of hairpin DNA **8** was 92%. The 5′-arm contained four sites of cleavage, including a strong site at 5′-GT_{14}-3′ (Figure 2.10A). The other sites were cleaved weakly in comparison, including sites at dinucleotide sequences 5′-AT_{10}-3′, 5′-GG_{12}-3′ and 5′-TA_{15}-3′. The 5′-GG_{12}-3′ is very interesting, representing one of the few sites of cleavage at a G residue and one of only two recorded 5′-GG-3′ cleavage sites within the library of hairpin DNAs. The 3′-arm of the hairpin DNA also had a site of cleavage at a 5′-GT-3′ dinucleotide sequence, but the 3′-arm also contained several cleavage sites in the flanking region of the hairpin DNA.

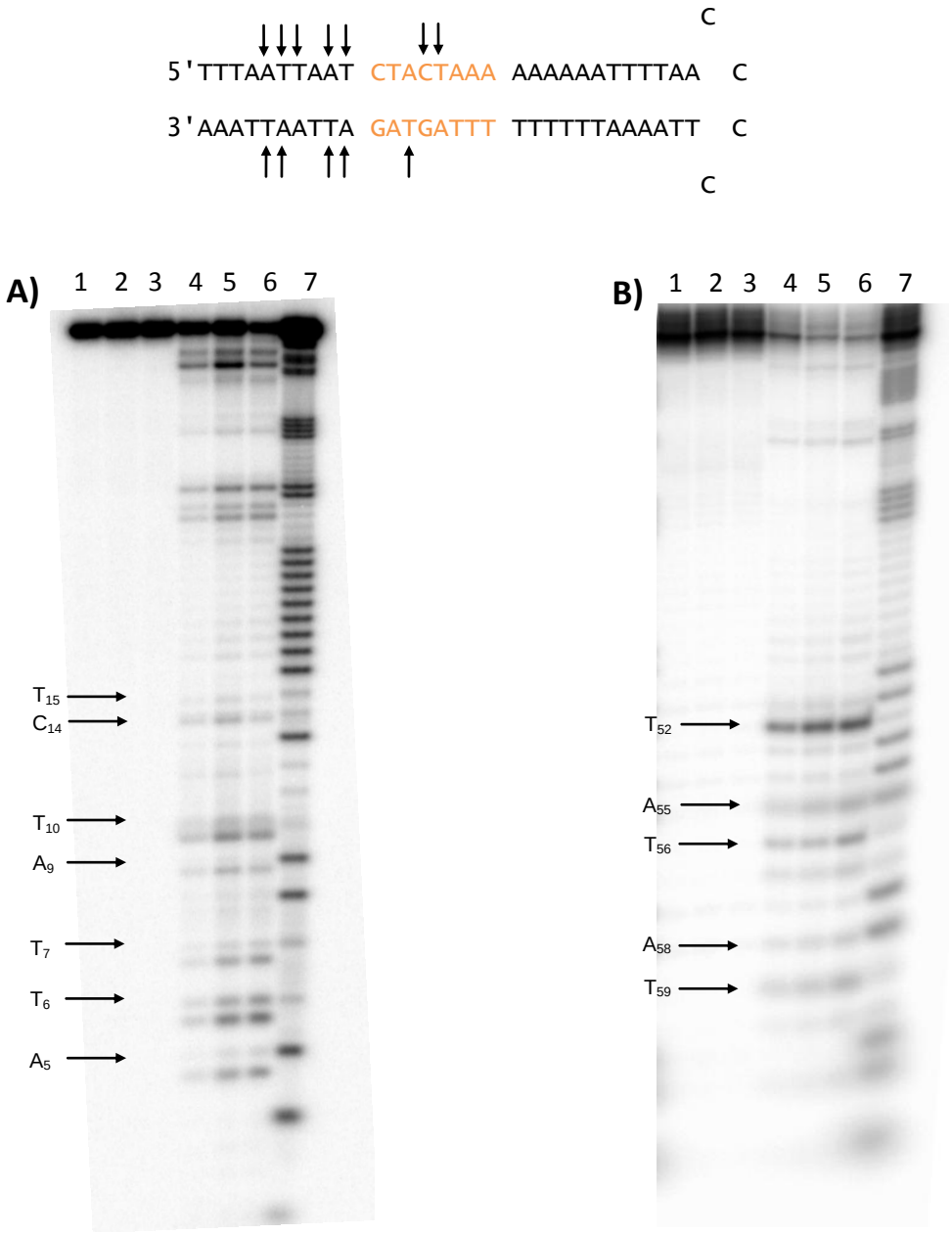

Figure 2.8: A) Sequence-selective cleavage of [5′-^{32}P]-end labeled 64-nt hairpin DNA **6** by BLM A_5. Lane 1, radiolabeled **6** alone; lane 2, 5 μM Fe^{2+}; lane 3, 5 μM BLM A_5; lane 4, 1 μM Fe(II) ·BLM A_5; lane 5, 2.5 μM Fe(II) ·BLM A_5; lane 6, 5 μM Fe(II) ·BLM A_5; lane 7, G+A lane. B) Sequence-selective cleavage of [3′-^{32}P]-end labeled 64-nt hairpin DNA **6** by BLM A_5. Lane 1, radiolabeled **6** alone; lane 2, 10 μM Fe^{2+}; lane 3, 5 μM BLM A_5; lane 4, 1 μM Fe(II) ·BLM A_5; lane 5, 2.5 μM Fe(II) ·BLM A_5; lane 6, 5 μM Fe(II) ·BLM A_5; lane 7, G+A lane.

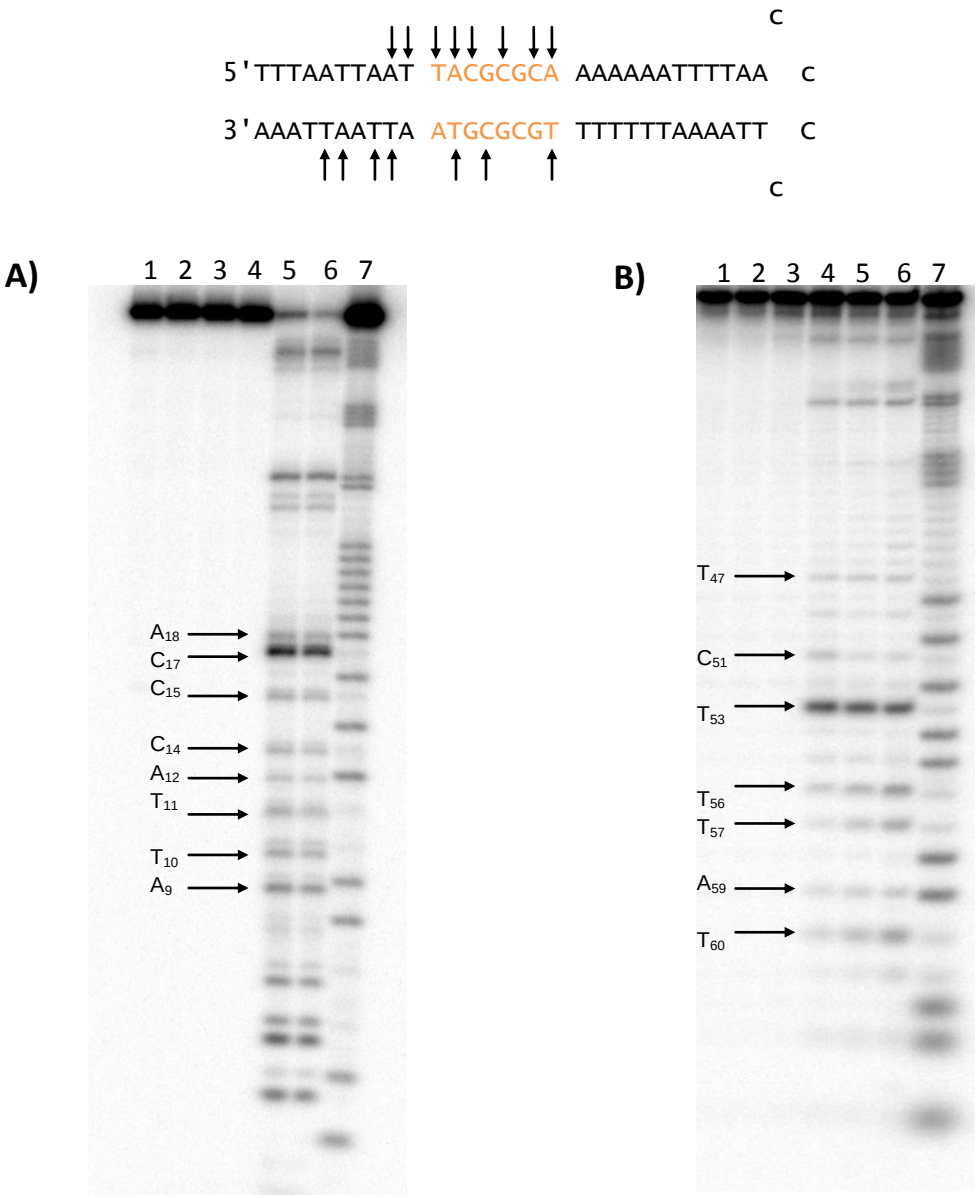

Figure 2.9: A) Sequence-selective cleavage of [5′-^{32}P]-end labeled 64-nt hairpin DNA **7** by BLM A_5. Lane 1, radiolabeled **7** alone; lane 2, 5 μM Fe^{2+}; lane 3, 5 μM BLM A_5; lane 4, 1 μM Fe(II) ·BLM A_5; lane 5, 2.5 μM Fe(II) ·BLM A_5; lane 6, 5 μM Fe(II) ·BLM A_5; lane 7, G+A lane. B) Sequence-selective cleavage of [3′-^{32}P]-end labeled 64-nt hairpin DNA **7** by BLM A_5. Lane 1, radiolabeled **7** alone; lane 2, 10 μM Fe^{2+}; lane 3, 5 μM BLM A_5; lane 4, 1 μM Fe(II) ·BLM A_5; lane 5, 2.5 μM Fe(II) ·BLM A_5; lane 6, 5 μM Fe(II) ·BLM A_5; lane 7, G+A lane.

The hairpin DNA **8** was cleaved six times on the 3′-arm of the hairpin DNA (Figure 2.10B). The strongest site of cleavage was at the 5′-GT_{50}-3′ dinucleotide sequence. Weaker sites included a site in the randomized region at 5′-AC_{52}-3′, and several sites in the invariant region: 5′-AT_{56}-3′, 5′-TT_{57}-3′, 5′-AA_{59}-3′ and 5′-AT_{60}-3′. This hairpin DNA contains 5′-GPy-3′ dinucleotide sequence per arm and they both represented the strongest site of cleavage on each arm of the hairpin DNA. The high binding specificity (97%) and relative paucity of preferred binding sites represent a notable example of binding and cleavage preference for BLM A_5.

The BLM-mediated cleavage sites resolved by 5′-^{32}P end labeling of hairpin DNA **9** are presented in Figure 2.11A. There were two cleaved dinucleotide sequences in the randomized region, both following the preferred sequence composition of BLM. The cleavage sites occurred at 5′-GT_{13}-3′ and 5′-GT_{16}-3′, with the former cleaved more extensively. Two other cleavage sites occurred in the invariant region at A_9 and T_{10}.

The randomized region of the 3′-arm of the hairpin DNA contained no canonical dinucleotide sequences for cleavage by BLM (Figure 2.11B). The strongest site of cleavage was the 5′-GA_{55}-3′ sequence. The 3′-arm of the hairpin DNA also showed stronger cleavage in the randomized region of the hairpin DNA than the 5′-arm. In summary, hairpin DNA **9** was bound with a specificity of 89% and cleaved a total of 11 times, including sites on both 3′ and 5′-arms of the hairpin DNA.

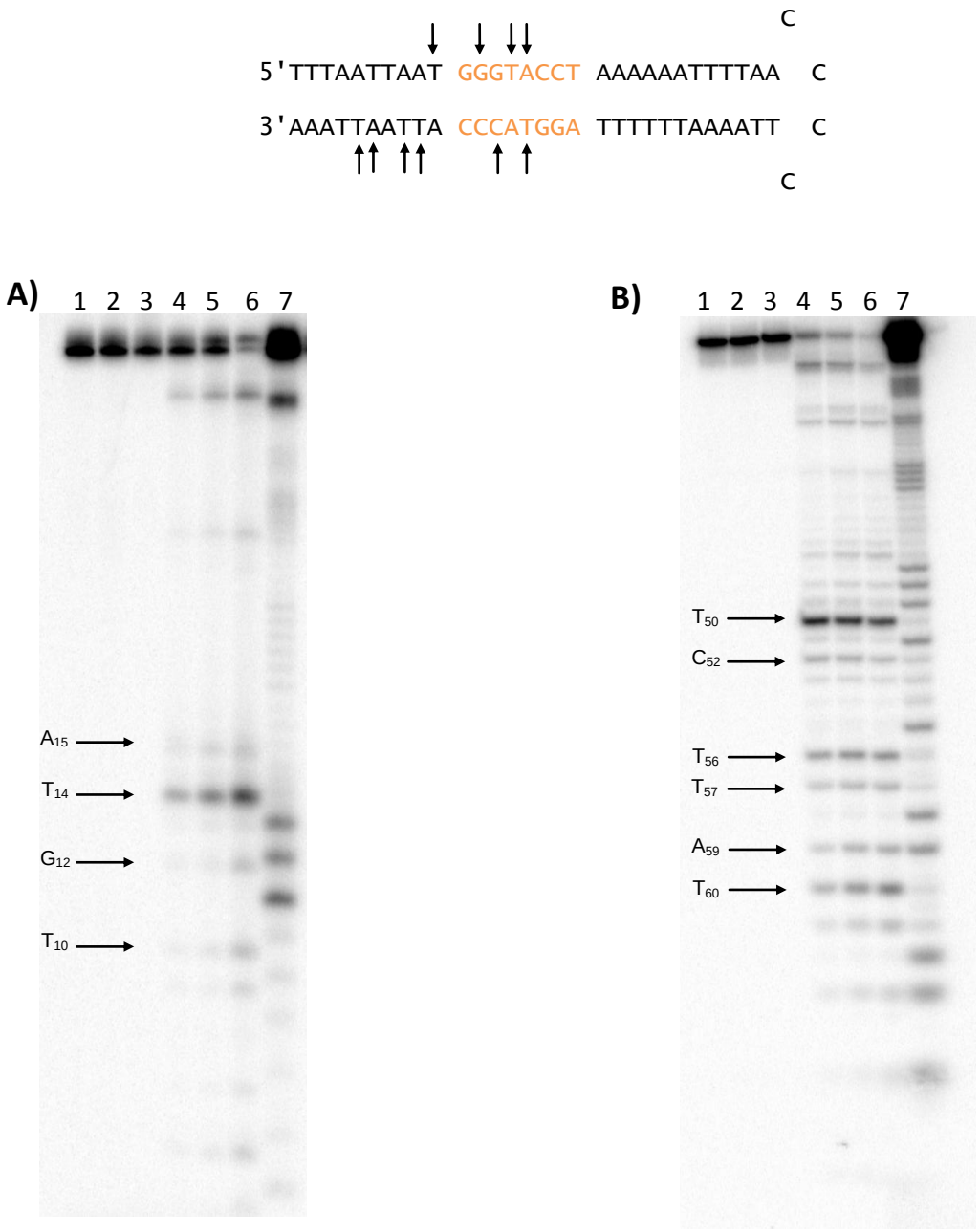

Figure 2.10: A) Sequence-selective cleavage of [5′-^{32}P]-end labeled 64-nt hairpin DNA **8** by BLM A_5. Lane 1, radiolabeled **8** alone; lane 2, 5 μM Fe^{2+}; lane 3, 5 μM BLM A_5; lane 4, 1 μM Fe(II) ·BLM A_5; lane 5, 2.5 μM Fe(II) ·BLM A_5; lane 6, 5 μM Fe(II) ·BLM A_5; lane 7, G lane.
B) Sequence-selective cleavage of [3′-^{32}P]-end labeled 64-nt hairpin DNA **8** by BLM A_5. Lane 1, radiolabeled **8** alone; lane 2, 10 μM Fe^{2+}; lane 3, 5 μM BLM A_5; lane 4, 1 μM Fe(II) ·BLM A_5; lane 5, 2.5 μM Fe(II) ·BLM A_5; lane 6, 5 μM Fe(II) ·BLM A_5; lane 7, G+A lane.

The site specific cleavage of 5′-^{32}P end labeled DNA **10** is presented in Figure 2.12A. BLM utilized five sites for cleavage on the 5′-arm of DNA **10** including 5′-AT_{10}-3′, 5′-GC_{13}-3′, an interesting 5′-CC_{14}-3′ dinucleotide sequence, as well as a 5′-TT_{17}-3′ and 5′-GA_{19}-3′. The 5′-CC-3′ dinucleotide sequence was not observed on any other hairpin DNA in this library, but it was cleaved inefficiently. The 5′-GC_{13}-3′ dinucleotide sequence represented the dominant cleavage site, as has been seen regularly on the hairpin DNAs that contain a cleavage site classically associated with Fe·BLM cleavage. Little cleavage was observed in the flanking region of this DNA, compared to other DNAs such as DNA **1** and **7**, which had considerable levels of cleavage compared to that within the randomized nucleotide sequence. The hairpin DNA **10** also had a comparable binding specificity to DNA **5**, but did not have sites preferred by BLM for cleavage. The lack of cleavage sites on the 5′-arm of the hairpin is contrasted by the eleven sites observed within the 3′-arm.

Similar to the 5′-arm, the 3′-arm had one canonical site of cleavage at 5′-GC_{53}-3′. This site and a variety of other sequence motifs were cleaved with comparable efficiency, including cleavage at 5′-GG_{52}-3′. There were four cleavage sites in the randomized region, but seven cleavage sites in the invariant region were observed for hairpin DNA **10**. For many of the 10 hairpin DNAs treated with BLM in this study, there was a difference between cleavage sites on the 5′- and 3′-arms.

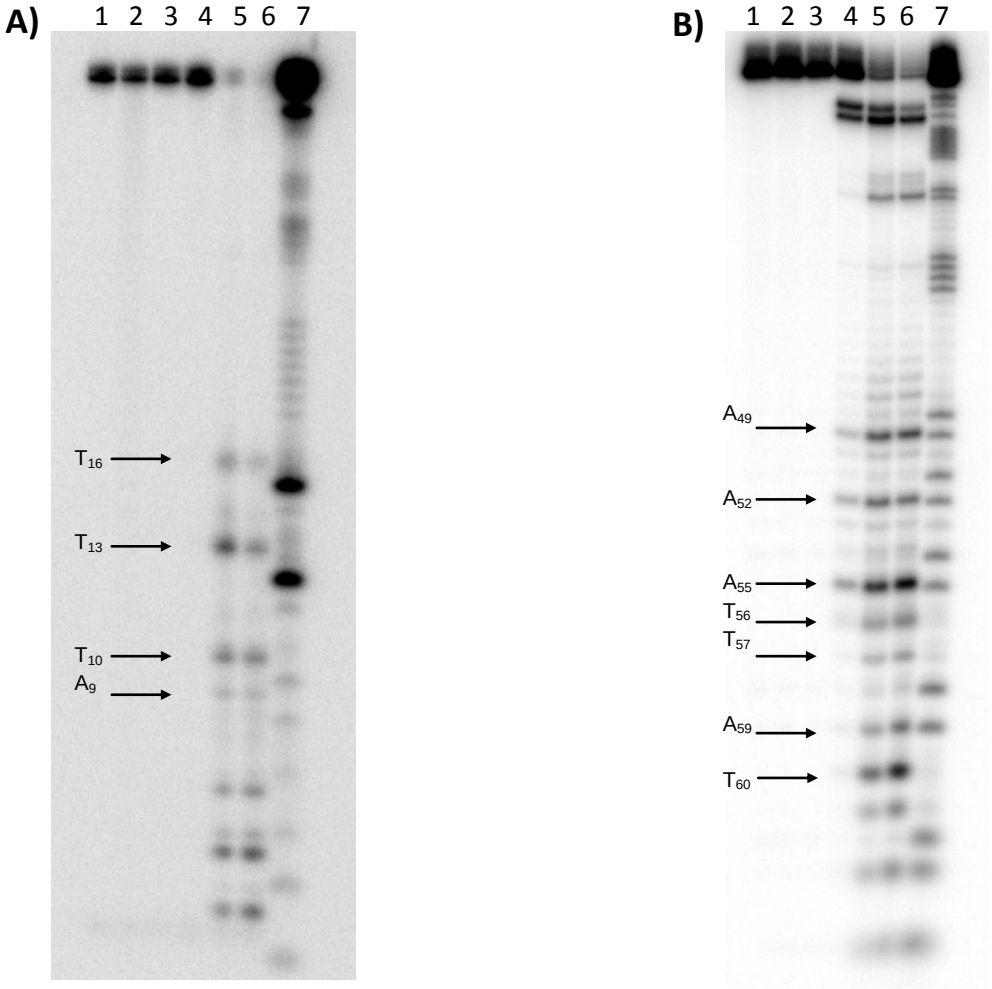

Figure 2.11: A) Sequence-selective cleavage of [5′-^{32}P]-end labeled 64-nt hairpin DNA **9** by BLM A_5. Lane 1, radiolabeled **9** alone; lane 2, 5 μM Fe^{2+}; lane 3, 5 μM BLM A_5; lane 4, 1 μM Fe(II) ·BLM A_5; lane 5, 2.5 μM Fe(II) ·BLM A_5; lane 6, 5 μM Fe(II) ·BLM A_5; lane 7, G lane.
B) Sequence-selective cleavage of [3′-^{32}P]-end labeled 64-nt hairpin DNA **9** by BLM A_5. Lane 1, radiolabeled **9** alone; lane 2, 10 μM Fe^{2+}; lane 3, 5 μM BLM A_5; lane 4, 1 μM Fe(II) ·BLM A_5; lane 5, 2.5 μM Fe(II)·BLM A_5; lane 6, 5 μM Fe(II) ·BLM A_5; lane 7, G+A lane.

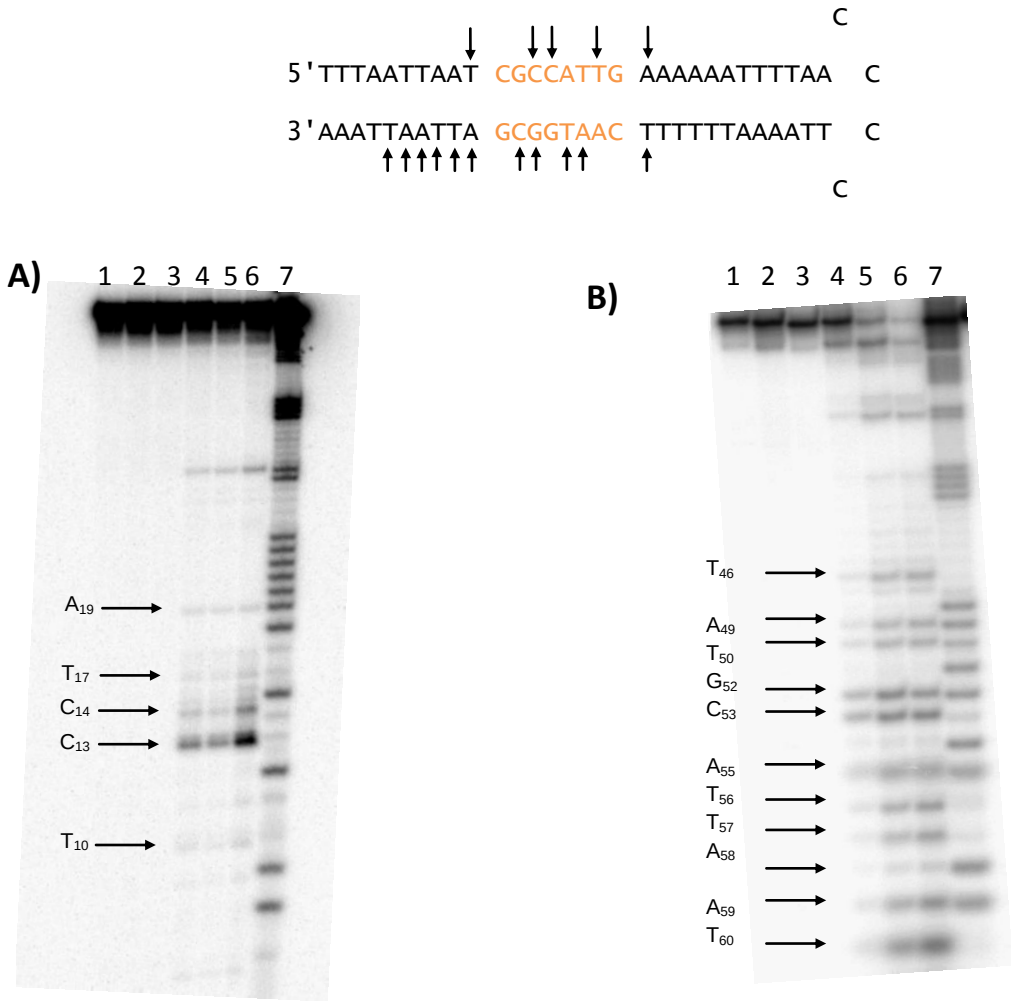

Figure 2.12: A) Sequence-selective cleavage of [5′-^{32}P]-end labeled 64-nt hairpin DNA **10** by BLM A_5. Lane 1, radiolabeled **10** alone; lane 2, 5 μM Fe^{2+};lane 3, 5 μM BLM A_5; lane 4, 1 μM Fe(II) ·BLM A_5; lane 5, 2.5 μM Fe(II) ·BLM A_5; lane 6, 5 μM Fe(II) ·BLM A_5; lane 7, G lane. B) Sequence-selective cleavage of [3′-^{32}P]-end labeled 64-nt hairpin DNA **10** by BLM A_5. Lane 1, radiolabeled **10** alone; lane 2, 10 μM Fe^{2+}; lane 3, 5 μM BLM A_5; lane 4, 1 μM Fe(II) ·BLM A_5; lane 5, 2.5 μM Fe(II)·BLM A_5; lane 6, 5 μM Fe(II) ·BLM A_5; lane 7, G+A lane.

Each hairpin differed in cleavage sites; however, the statistical analyses of cleavage sites mediated by BLM on the hairpin DNA library showed that, in the aggregate, the 3′ and 5′-arms had a similar number of cleavage sites between A_5 and A_{19}. The 15-nt range represented the extreme positions of BLM-mediated cleavage on the hairpin DNAs when 5′-^{32}P end labeled. Table 2.3 shows the number of cleavages and at which dinucleotide sequence the cleavages occurred on the 5′-arm. The data in Tables 2.4 shows the number of dinucleotide cleavages available and the percentage at which they were cleaved on the 5′-arm. The most prevalent dinucleotide sequence cleaved in this region was 5′-AA-3′, occurring 28 times. However, it was only cleaved 36% of the time. The most cleaved dinucleotide sequence was 5′-AT-3′. BLM mediated cleavage at this sequence 56% of the time it occurred within the specified sequence range on the 5′-arm of the hairpin DNA. Interestingly, preferred sequences nine preferred sequences of cleavage (5′-GPy-3′) were selected 100% of the time. The 5′-GA-3′ was also cleaved every time it appeared within the sequence space specified on the 5′-arm.

On the 3′-arm of the hairpin DNA library, the range of BLM mediated cleavage spanned T_{46} to T_{61}, inclusively (Tables 2.5 and 2.6). BLM mediated cleavage on the 3′-arm showed more efficient cleavage at 5′-AT-3′ dinucleotide sequences, but surprisingly lower efficiency at a canonical dinucleotide sequence preferred for cleavage by BLM. Dinucleotide sequence 5′-GC-3′ appeared four times and was subject to BLM mediated cleavage three times (75% cleavage efficiency). Dinucleotide sequences 5′-GT-3′ and 5′-GA-3′ were cleaved each

time they occurred within the sequence space on the 3′-arm as recorded for the 5′-arm of the hairpin DNAs.

Table 2.3: DNAs **1**-**10** are summarized by the dinucleotide sequences cleaved by BLM A_5 in a 5′-^{32}P end labeled cleavage assay. The total number of cleavages per DNA is shown on the right hand side, which is then totaled at the bottom.

5′-XX-3′	DNA Hairpins										
	1	2	3	4	5	6	7	8	9	10	total
AA	1	1	1	1	1	1	1		1	2	10
AC					1	1	1				3
AG											0
AT	3	1	1	2	1	1	1	1	1	2	14
CA							1				1
CC										1	1
CG											0
CT						1					1
GA	2	1	1	3	1					1	9
GC		1					2			1	4
GG								1			1
GT		1	1					1	2		5
TA			2				1	1			4
TC											0
TG											0
TT					1	1				1	3
											56

In summary, on both 3′ and 5′-arms, 5′-AT-3′ dinucleotide was the most often cleaved site. This site is generally not preferred for cleavage by BLM, but this library of hairpin DNAs contains many AT sequences, which BLM cleaved roughly 65% of the time the dinucleotide sequence appeared on both 3′ and 5′-arms. There were 111 sites of cleavage on these 10 hairpins including both the 3′ and 5′-arms, approximately one third of which were 5′-AT-3′ dinucleotide

sequences. Interestingly, the 5′-AG-3′ dinucleotide sequence was not cleaved at all in this library of 10 hairpin DNAs. Although this does not necessarily indicate that this sequence cannot be cleaved, finding a hairpin DNA where the sequence 5′-AG-3′ is cleaved would be interesting in that it would enable an understanding of the surrounding sequence composition permitting cleavage at that position.

Table 2.4: The number of times a dinucleotide sequences appears on the 5′-arm of a hairpin between A_5 and A_{19}, inclusively. This sequence space represents the extreme range of BLM mediated cleavage on the 5′-arm of the hairpin DNA.

5′-XX-3′	DNA Hairpin												
	1	2	3	4	5	6	7	8	9	10	Occurrences	Cleavages	Percent cleaved
AA	2	2	3	2	4	5	3	2	3	2	28	10	36%
AC		1			1	1	1	1			5	3	60%
AG	1		1	2	1						5	0	0%
AT	4	2	2	3	3	2	2	2	2	3	25	14	56%
CA	1	1			1		1			1	5	1	20%
CC								1		1	2	1	50%
CG		2					2		1	1	6	0	0%
CT						2		1			3	1	33%
GA	2	1	1	3	1					1	9	9	100%
GC		1					2			1	4	4	100%
GG			2	1				2			5	1	20%
GT		1	1					1	2		5	5	100%
TA	2	1	2	2	3	3	2	3	2	1	21	4	19%
TC	1	1				1			1	1	5	0	0%
TG	1	1	1	1				1	1	1	7	0	0%
TT	1	1	2	1	1	1	2	1	3	2	15	3	20%

Table 2.5: DNAs **1**-**10** are summarized by the dinucleotide sequences cleaved by BLM A_5 in a 3′-^{32}P end labeled cleavage assay. The total number of cleavages per DNA is shown on the right hand side, which is then totaled at the bottom.

5′-XX-3′	Hairpin DNA										
	1	2	3	4	5	6	7	8	9	10	total
AA	1		1				1		3	2	8
AC								1			1
AG											0
AT	4		2	1	2	2	2	1	2	3	19
CA											0
CC											0
CG											0
CT				2							2
GA	1	1				1			1	1	5
GC		1					1			1	3
GG										1	1
GT		1			1	1	1	1			5
TA										1	1
TC											0
TG											0
TT	2	1	2				2		1	2	10
											55

DsDNA damage mediated by BLM on the Hairpin DNA Library

The characterization of dsDNA damage has been an important priority in BLM studies due to the belief that it may be the mechanism through which BLM exerts its cytotoxicity. The Povirk laboratory was the first to present rules for this cleavage, which are described in Chapter 1. In order to characterize this hairpin DNA library for its propensity to undergo dsDNA cleavage by BLM A_5, the method of native polyacrylamide gel analysis followed by sequencing at putative dsDNA damage sites on a denaturing gel was employed. In order to provide proof

of concept for this method when applied to the hairpin DNAs, DNA **8** was first subjected to this method of characterization. DNA **8** contains a well known self complementary $d(GTAC)_2$ sequence which is a studied, high efficiency site for dsDNA cleavage by BLM.[66]

Table 2.6: The number of times a dinucleotide sequences appears on the 3′-arm of a hairpin between T_{46} and T_{61}, inclusively. This sequence space represents the extreme range of BLM mediated cleavage on the 3′-arm of the hairpin DNAs.

5′-XX-3′	Hairpin DNA												
	1	2	3	4	5	6	7	8	9	10	occurrences	cleavages	percent cleaved
AA	1	1	2	1	1	1	2	1	3	2	15	8	53%
AC	-	1	1	-	-	-	-	1	2	-	5	1	20%
AG	-	-	-	-	-	2	-	1	-	-	3	0	0%
AT	4	2	2	3	4	2	2	2	2	3	26	19	73%
CA	1	1	1	1				1	1	1	7	0	0%
CC			2	1				2			5	0	0%
CG		2					2		1	1	6	0	0%
CT	1		1	2	1						5	2	40%
GA	1	1				1			1	1	5	5	100%
GC		1					2			1	4	3	75%
GG								1		1	2	1	50%
GT		1			1	1	1	1			5	5	100%
TA	2	1	2	2	3	3	2	3	2	1	21	1	5%
TC	2	1	1	3	1					1	9	0	0%
TG	1	1			1		1			1	5	0	0%
TT	3	3	4	3	4	6	4	3	4	3	37	10	27%

Figure 2.13 displays the results of treating 5′ and 3′-^{32}P end labeled hairpin DNA **8** and separating the reaction mixture on a native polyacrylamide gel. Both the A and B bands comigrated, and the weaker lower running C and D bands also comigrated (Figure 2.13). These bands were both excised from the

polyacrylamide and electrophoresed on a denaturing gel with a sequencing ladder to characterize the sites of damage. Figure 2.14 shows plainly that d(GTAC) sequence was indeed cleaved in dsDNA fashion by BLM at T_{14} and T_{50} and produced a 5′-extension on the 3′-arm of the hairpin DNA, according to electrophoresis of spots A and B, respectively. These results are consistent with the results published previously, [67] and indicate that this method can be applied to the hairpin DNA library for characterizing the sequences putatively cleaved twice by one molecule of Fe·BLM A_5.

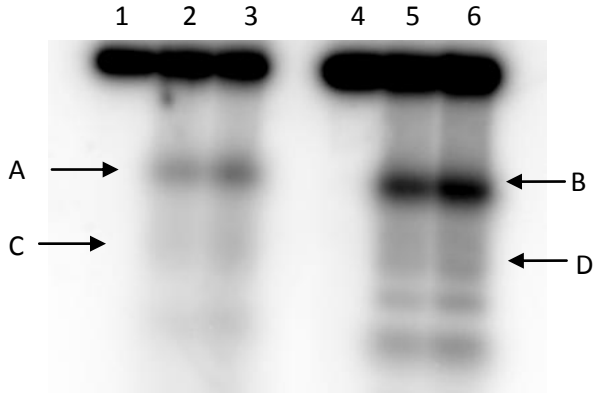

Figure 2.13: Cleavage products of DNA **8** resolved by native polyacrylamide electrophoresis. Lanes 1 – 3 contain [3′-^{32}P]-end labeled 64-nt hairpin DNA **8**. Lanes 4 – 6 contain [5′-^{32}P]-end labeled 64-nt hairpin DNA **8**. Lane 1, [3′-^{32}P]-end labeled 64-nt hairpin DNA **8** alone; lane 2, 1.5 μM Fe(II)·BLM A_5; lane 3, Fe(II)·BLM A_5 3.0 μM; lane 4, [5′-^{32}P]-end labeled 64-nt hairpin DNA **8** alone; lane 5, 1.5 μM Fe(II)·BLM A_5; lane 6, Fe(II)·BLM A_5 3.0 μM

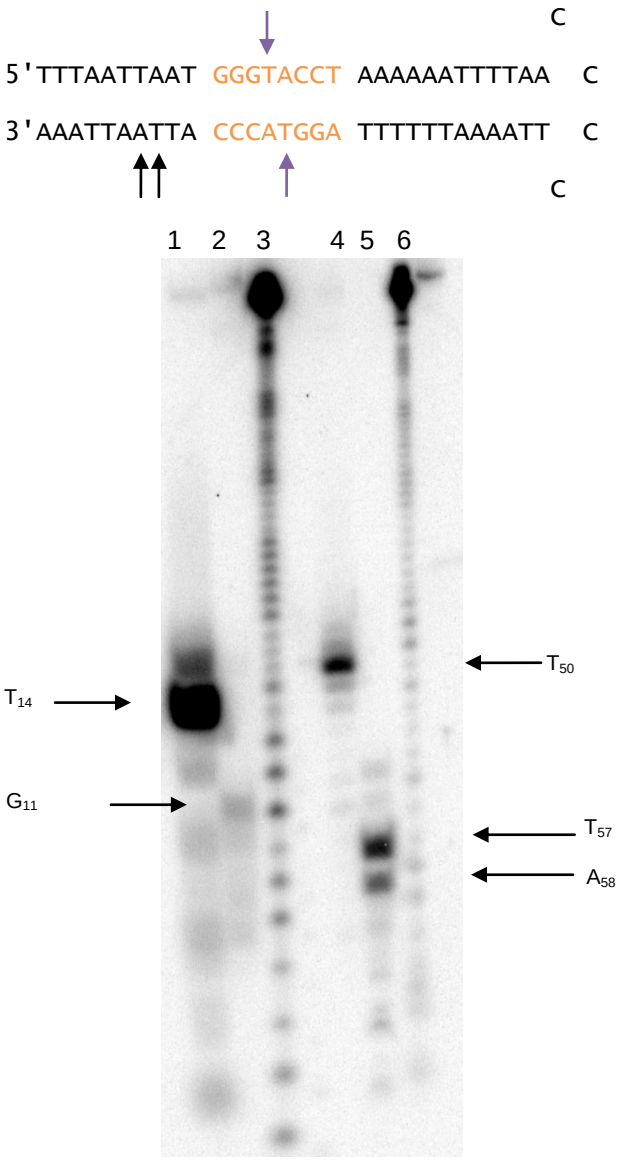

Figure 2.14: Denaturing polyacrylamide electrophoresis of spots A, B, C and D from the gel pictured in Figure 2.13. Lane 1, spot A; lane 2, spot C; lane 3, [5′-^{32}P]-end labeled 64-nt hairpin DNA **8** G+A lane; lane 4, spot B; lane 5, spot D; lane 6, [3′-^{32}P]-end labeled 64-nt hairpin DNA **8** G+A lane. The purple arrows indicate linked cleavage events.

Discussion

Bleomycin has been studied extensively for several decades, and has been in clinical use for nearly as long. Even so, many facets of the action of BLM are not completely understood, as evidenced by the present study and the foundational works preceding it.[7,60] The relationship between DNA binding of BLM and its cleavage of DNA was examined using a specially identified library of 64-nt hairpin DNAs which were selected from a random hairpin DNA library via a SELEX-type procedure. This library provides a sequence space of 65, 536 possible combinations.[60] The present work differs from previous studies in other laboratories, which have used arbitrarily chosen DNA substrates in reactions with BLM at high BLM:DNA ratios. The experimental conditions applied in the aforementioned studies are inconsistent with the clinical administration of the drug. It is used in treatment in amounts where the concentration of DNA present is far in excess of BLM.

The present study has characterized 10 of these DNAs using both 3′ and 5′ -^{32}P end labeling to permit measurement of the cleavage sites from the entirety of the hairpin DNAs **1**-**10** with BLM. The goal is to identify DNA sequence elements preferred for cleavage in substrates strongly bound by BLM to analyze the obligatory binding step that occurs before C-4′ H abstraction. Study of the hairpin DNAs through cleavage site analysis has shown that they are all substrates for BLM cleavage, although some were cleaved more avidly than others. The hairpin DNAs also showed sites of cleavage that are not traditionally found in

DNA cleavage reactions with BLM, including cleavage in the AT-rich invariant regions of the hairpin DNA.

Overall, the 10 DNAs contained 111 sites that could be cleaved by BLM, while the amount of cleavage per DNA molecule varied from three sites on DNA **8** (Figure 2.10A) to 15 on DNA **5** (Figure 2.7B), in 5′ and 3′-^{32}P end labeling experiments, respectively. Hairpin DNAs **3** (Figure 2.5) and **4** (Figure 2.6) differed in the amounts and relative intensities of cleavage sites between their 5′ and 3′-arms. Hairpin DNA **3** perhaps offered the most interesting results: the 5′-arm contained six cleavage sites that only became apparent at 20 μM concentration of Fe·BLM A_5 (Figure 2.5B). The 3′-arm showed no cleavage inside the randomized region and a small amount of cleavage at sites not usually cleaved by Fe·BLM in the invariant flanking AT-rich sequence regions. Considering the low binding specificity (76%), the lack of cleavage in the randomized region indicates BLM–DNA binding is an important determinant of cleavage efficiency. DNA **4** also supports the importance of binding specificity in determining the number of DNA sites cleaved and the efficiency of DNA cleavage.

DNA **4** showed a similar result, a cleaved 5′-arm with a G-rich sequence, but no canonical cleavage motifs (Figure 2.6A). Even still, the DNA is cleaved more strongly and at more sites than on the 3′-arm, which is pyrimidine rich. The coincident lack of 3′-arm cleavage sites and relatively low binding specificity indicate that BLM binding preference can be dictated by the sequence of one strand in a DNA duplex, and comparable cleavage on both strands of the duplex is

not guaranteed. The specific structural elements themselves are not determined at this time; however, the most poorly bound DNAs tend to have very few G residues in their sequence and the least amount of cleavage. Although, the converse is not necessarily true. The high binding specificity of hairpin DNA **2** is lacking in cleavage sites, achieving only three on the 5′-arm and four on the 3′-arm (Figure 2.4).

DNA **2** had four strong cleavage sites of the type 5′-GPy-3′ and the highest binding specificity (97%). The strongest relative cleavage occurred at 5′-GT_{13}-3. This efficient cleavage at few sites on both strands while offering the highest binding specificity indicates a predilection for BLM to preferentially bind a short sequence motif strongly and cleave preferentially at those sites. It is also possible, however, that many sites on the hairpin were bound, but the hairpin DNA **2** was simply not cleaved at those sites.

DNA **5** provided a stark contrast to the other DNAs studied. It contains no canonical sites for cleavage, but was still cleaved by BLM 13 times on the 5′-arm (Figure 2.7B). The BLM mediated cleavages occurred in both the randomized and invariant regions. The binding specificity of DNA **5** was 90%, which is relatively high, but not the greatest measured. The coincidence of a high binding specificity and a great number of cleavage sites could indicate that BLM responds to the tertiary structure assumed by this hairpin DNA where it is able to make many contacts with the molecule. Unlike DNA **2** (Figure 2.4), which had comparatively few sites of cleavage and a higher binding specificity, DNA **5** (Figure 2.7) may bind less tightly, allowing for interaction sufficient for cleavage activity, but

indiscriminate enough that BLM binding and cleavage events occur at many points on the DNA molecule.

The idea that BLM identifies a global DNA structure is supported by the cleavage pattern demonstrated by the 3′-^{32}P end labeled DNA **1** (Figure 2.3B). More cleavage appeared in the invariant region of this DNA than in the others tested. BLM may recognize the minor groove of this hairpin DNA more readily in the invariant than in the randomized region. Precisely what these recognition elements are is uncertain, but if the randomized region is lacking in preferred sites, the BLM molecule may bind readily to the deeper minor groove of the AT-rich region such that its opportunity to cleave within that region is enhanced compared to the 8-bp randomized region. Also of note is that thymidine was the preferred nucleoside to cleave in the randomized region, following the usual preference of BLM to oxidatively release pyrimidine bases and base propenals.

The analysis of Fe·BLM cleavage of this specially selected library of hairpin DNAs shows that binding is an important step in the determination of the DNA sequences cleaved by BLM. This library is rich in non-traditional cleavage sites and the 64-nt hairpin DNAs were greatly preferred over the 16-nt hairpin DNA as a substrate for binding. The hairpin DNAs also offer insights into the strand selectivity of BLM, where a molecule can be a substrate for cleavage, but one strand is preferred greatly over the other, as in the G content of one arm of the hairpin DNA versus the other.

The development and characterization of this library through cleavage reactions represents an important step forward in delineating the relationship

between binding and cleavage to binding of DNA. These results, in concert with preliminary double-stranded damage assays indicate quite strongly that binding specificity may be a major determinant in how BLM acts *in vivo*. The exact DNA structures and precise motifs that BLM prefers, however, are still elusive and worthy of further study. Possible avenues for future work include employing a more iterative SELEX-type procedure along with a larger randomized region for binding by BLM.

The method developed for studying the dsDNA damage inflicted by BLM A_5 on DNA **8** is convenient for the identifying sites of dsDNA, but is a poor method for characterization of ssDNA:dsDNA damage ratios (Figures 2.10, 13 and 14). Both the sites of cleavage and the rates at which BLM A_5 produces either ssDNA damage or dsDNA are of interest. However this method is only applicable to finding the sites of dsDNA damage.

The finding that many of these strongly bound hairpin DNAs are subject to dsDNA damage at multiple sites would offer more insight into the importance of binding selectivity to BLM–mediated cleavage. The exact sequence motif(s) and global structures that facilitate the production of dsDNA damage are certainly worthy of further study. Direct and unambiguous measurement of the extent of ds versus ss damage in such small DNAs presents a technical challenge that will require the development of another assay system.

Experimental Procedures

Terminal deoxynucleotidyl transferase was purchased from Roche Applied Science. T4 polynucleotide kinase was obtained from New England Biolabs. All synthetic oligonucleotides, purified by ion exchange, were purchased from Integrated DNA Technologies. Radionucleotides were purchased from Perkin Elmer Life Sciences. BLM A_5 solutions were dissolved in water immediately prior to use. $Fe(NH_4)_2(SO_4)_2 \cdot 6H_2O$ was purchased from Sigma Aldrich Chemicals and used to prepare fresh Fe^{2+} solutions immediately prior to use. Chelex 100 was purchased from Sigma Aldrich and used to remove adventitious Fe^{2+} from solutions prior to experiments.

Polyacrylamide gel electrophoresis was carried out in 90 mM Tris-borate buffer, pH 8.3, containing 5 mM EDTA. Cleavage sites were confirmed by comparison with the reaction products obtained by the Maxam-Gilbert G lane, Maxam-Gilbert G + A[67] and cytidine specific sequencing protocols.[68] Analysis of the polyacrylamide gels was carried out by phosphorimager analysis using a Molecular Dynamics Storm 820 Phosphorimager.

3′-^{32}P End Labeling and Purification of 64-nt Hairpin DNAs

3′-^{32}P end labeling was carried out by combining 10 pmol of the appropriate 64-nt hairpin DNA, 0.06 mCi [α-^{32}P]cordycepin (specific activity 5000 Ci (185 TBq)/mmol) and 400 units of recombinant terminal transferase in 40 µL (total volume) of 25 mM Tris-HCl, pH 6.6, containing 200 mM potassium cacodylate, 2.5 mM $CoCl_2$ and 0.25 mg/mL BSA. The reaction mixture was

incubated at 37 °C for 1 h. The 3′-^{32}P end labeled 64-nt hairpin DNA was purified by 16% polyacrylamide gel electrophoresis at 1800 V for 2.5 h.

5′-^{32}P End Labeling and Purification of Hairpin DNA

Ten pmol of 64-nt hairpin DNA was 5′-^{32}P end labeled by incubation with 20 units of T4 polynucleotide kinase and 0.06 mCi [γ-^{32}P]ATP (specific activity 6000 Ci (222 TBq)/mmol) in 50 μL (total volume) of 70 mM Tris-HCl buffer, pH 7.6, containing 10 mM $MgCl_2$ and 5 mM dithiothrietol. The reaction mixture was incubated at 37 °C for 1 h followed by heat inactivation of the enzyme at 65 °C for 20 min. The 5′-^{32}P end labeled 64-nt hairpin DNA was purified by 16% polyacrylamide gel electrophoresis at 1800 V for 2.5 h.

Sequence-Selective Cleavage of Radiolabeled Hairpin DNA by BLM A_5

A sample of 5′ or 3′-^{32}P end labeled hairpin DNA (50,000 cpm) was treated with the appropriate concentrations of Fe^{2+} and BLM solutions in 5 μL (total volume) of 10 mM Na cacodylate buffer, pH 7.0. Reactions were incubated at 25 °C for 30 min followed by removal of the supernatant under diminished pressure. Ten μL of denaturing gel loading buffer containing 98% formamide, 2 mM EDTA, 0.25% (w/v) bromophenol blue and 0.25% (w/v) xylene cyanol was added to the DNA pellet. The resulting solution was heated at 90 °C for 10 min, followed by chilling on ice. Five microliters of each sample was loaded onto a denaturing gel (16% polyacrylamide, 7 M urea) and run at 50 W for 2.5 h. Gels were visualized using a phosphorimager.

Polyacrylamide Electrophoresis of 64-nt Hairpin DNAs for dsDNA Damage

A sample of ^{32}P end labeled hairpin DNA (50,000 cpm) was treated with the appropriate concentrations of Fe^{2+} and BLM solutions in 5 μL (total volume) of 10 mM Na cacodylate buffer, pH 7.0 containing 2 mM $MgCl_2$. The reactions were quenched by addition of 1 μL native gel loading buffer containing 40% (w/v) sucrose, 0.25% (w/v) bromophenol blue and 0.25% (w/v) xylene cyanol and immediately electrophoresed on a native polyacrylamide gel (20% polyacrylamide) incubated at 4 °C run at 240 V for 18 h.

After visualization via phosphorimager, relevant bands were excised from the gel and incubated at 37 °C in 1 mL of ddH_2O for 18 h. After decantation, the sample was concentrated to ~5 μL under diminished pressure. Ten µL of denaturing gel loading buffer containing 98% formamide, 2 mM EDTA, 0.25% (w/v) bromophenol blue and 0.25% (w/v) xylene cyanol was added to the resulting solution. The mixture was heated at 90 °C for 10 min and the sample and an appropriate Maxam-Gilbert sequencing ladder were loaded onto a denaturing gel (16% polyacrylamide, 7 M urea) and run at 50 W for 2.5 h. The gel was visualized using a phosphorimager.

REFERENCES

(1) Dahm, R. *Human Genet.* **2008**, *122*, 565.

(2) Stryer, L. *Biochemistry, 3rd ed.* W.H. Freeman and Company: New York, 1988.

(3) Watson, J. D.; Crick, F. H. C. *Nature* **1953**, *171*, 737.

(4) Gates, K. S. *Chem. Res. Toxicol.* **2009**, *22*, 1747.

(5) Hershey, A. D.; Chase, M. *J. Gen. Physiol.* **1952**, *36*, 39.

(6) Block, J. H.; Beale, J. M. *Wilson and Gisvold's Textbook of Organic Medicinal and Pharmaceutical Chemistry*; 11th ed. Lippincott Williams & Wilkins: Philadelphia, 2004.

(7) Giroux, R. A.; Hecht, S. M. *J. Am. Chem. Soc.* **2010**, *132*, 16987.

(8) Umezawa, H.; Suhara, Y.; Takita, T.; Maeda, K. *J. Antibiot. (Tokyo)* **1966**, *19*, 210.

(9) Wit, R. de; Stoter, G.; Kaye, S. B.; Sleifer, D. T.; Jones, W. G.; Huinink, W. W. t B.; Rea, L. A.; Collette, L.; Sylvester, R. *J. Clin. Oncol.* **1997**, *15*, 1837.

(10) Aridgides, P.; Bogart, J.; Shapiro, A.; Gajra, A. *Advances in hematology* **2011**, 309.

(11) Stubbe, J.; Kozarich, J. W. *Chem. Rev.* **1987**, *87*, 1107.

(12) Carter, B. J.; Vroom, E. de; Long, E. C.; Marel, G. A. van der; Boom, J. H. van; Hecht, S. M. *Proc. Natl. Acad. Sci. U.S.A.* **1990**, *87*, 9373.

(13) Sausville, E. A.; Peisach, J.; Horwitz, S. B. *Biochemistry* **1978**, *17*, 2740.

(14) Hecht, S. M. *Fed. Proc.* **1986**, *45*, 2784.

(15) Steighner, R. J.; Povirk, L. F. *Proc. Natl. Acad. Sci. U.S.A.* **1990**, *87*, 8350.

(16) Chen, J.; Stubbe, J. *Nat. Rev.* **2005**, *5*, 102.

(17) Boggs, S. S.; Sartiano, G. P.; DeMezza, A. *Cancer Res.* **1997**, *34*, 1974.

(18) Hecht, S. M. *J. Nat. Prod.* **2000**, *63*, 158.

(19) Kilkuskie, R.E.; Suguna, H.Y.; Murugesan, N.; Hecht, S. M. *Proc. Natl. Acad. Sci. U.S.A.* **1985**, *107*, 260.

(20) Goodwin, K. D.; Lewis, M. a; Long, E. C.; Georgiadis, M. M. *Proc. Natl. Acad. Sci. U.S.A.* **2008**, *105*, 5052.

(21) Murugesan, N.; Ehrenfeld, G. M.; Hecht, S. M. *J. Biol. Chem.* **1982**, *257*, 8600.

(22) Ehrenfeld, G. M.; Murugesan, N.; Hecht, S. M. *Inorg. Chem.* **1984**, *23*, 1496.

(23) Heimbrook, D. C.; Carr, S. A.; Mentzer, M. A.; Long, E. C.; Hecht, S. M. *Inorg. Chem.* **1987**, *26*, 3835.

(24) Akkerman, M. J.; Haasnoot, C. G.; Hilbers, C. W. *Eur. J. Biochem.* **1988**, *173*, 211.

(25) Shipley, J. B.; Hecht, S. M. *Chem. Res. Toxicol.* **1988**, *1*, 25.

(26) Burger, R. M. *Chem. Rev.* **1998**, *98*, 1153.

(27) Sugiyama, H.; Kilkuskie, R. E.; Chang, L. H.; Ma, L. T.; Hecht, S. M.; Marel, G. A. van; der Boom, J. H. van. *J. Am. Chem. Soc.* **1986**, *108*, 3852.

(28) Sucheck, S. J.; Ellena, J. F.; Hecht, S. M. *J. Am. Chem. Soc.* **1998**, *120*, 7450.

(29) Abraham, A. T.; Zhou, X.; Hecht, S. M. *J. Am. Chem. Soc.* **2001**, *123*, 5167.

(30) Povirk, L. F.; Hogan, M.; Dattagupta, N. *Biochemistry* **1979**, *18*, 96.

(31) Boger, D. L.; Cai, H. *Angew. Chem.* **1999**, *38*, 448.

(32) Boger, D. L.; Honda, T.; Menezes, R. F.; Colletti, S. L. *J. Am. Chem. Soc.* **1994**, *116*, 5631.

(33) Ma, Q.; Xu, Z.; Schroeder, B. R.; Sun, W.; Wei, F.; Hashimoto, S.; Konishi, K.; Leitheiser, C. J.; Hecht, S. M. *J. Am. Chem. Soc.* **2007**, *129*, 12439.

(34) Rishel, M. J.; Thomas, C. J.; Tao, Z. F.; Vialas, C.; Leitheiser, C. J.; Hecht, S. M. *J. Am. Chem. Soc.* **2003**, *125*, 10194.

(35) Boger, D. L.; Colletti, S. L.; Teramoto, S.; Ramsey, T. M.; Zhou, J. *Bioorg. Med. Chem.* **1995**, *3*, 1281.

(36) Boger, D. L.; Teramoto, S.;Honda, T.; Zhou, J. *J. Am. Chem. Soc.* **1995**, *117*, 7338.

(37) Boger, D. L.; Colletti, S. L.; Honda, T.; Menezes, R. F. *J. Am. Chem. Soc.* **1994**, *116*, 5607.

(38) Bailly, C.; Kenani, M. J.; Waring, M. J. *FEBS Lett.* **1995**, *372*, 144.

(39) Oppenheimer, N. J.; Rodriguez, L. O.; Hecht, S. M. *Proc. Natl. Acad. Sci. U.S.A.* **1979**, *76*, 5616.

(40) Oppenheimer, N. J.; Chang, C.; Chang, L. H.; Ehrenfeld, G.; Rodriguez, L. O.; Hecht, S. M. *J. Biol. Chem.* **1982**, *257*, 1606.

(41) Chapuis, J. C.; Schmaltz, R. M.; Tsosie, K. S.; Belohlavek, M.; Hecht, S. M. *J. Am. Chem. Soc.* **2009**, *131*, 2438.

(42) Thomas, C. J.; McCormick, M. M.; Vialas, C.; Tao, Z. F.; Leitheiser, C. J.; Rishel, M. J.; Wu, X.; Hecht, S. M. *J. Am. Chem. Soc.* **2002**, *124*, 3875.

(43) Burger, R. M.; Kent, T. A.; Horwitz, S. B.; Munck, E.; Peisach, J. *J. Biol. Chem.* **1983**, *258*, 1559.

(44) Burger, R. M.; Peisach, J.; Horwitz, S. B. *J. Biol. Chem.* **1981**, *256*, 11636.

(45) Decker, A.; Chow, M. S.; Kemsley, J. N.; Lehnert, N.; Solomon, E. I. *J. Am. Chem. Soc.* **2006**, *128*, 4719.

(46) Sugiyama, H.; Kilkuskie, R. E.; Hecht, S. M. *J. Am. Chem. Soc.* **1985**, *107*, 7765.

(47) Sugiyama, H.; Xu, C.; Murugesan, N.; Hecht, S. M. *J. Am. Chem. Soc.* **1985**, *107*, 4104.

(48) Giese, B.; Beyrich-Graf, X.; Erdmann, P.; Giraud, L.; Imwinkelried, P.; Mueller, S. N.; Schwitter, U. *J. Am. Chem. Soc.* **1995**, *117*, 6146.

(49) Sugiyama, H.; Xu, C.; Murugesan, N.; Hecht, S. M.; Marel, G. A. van der; Boom, J. H. van. *Biochemistry* **1988**, *27*, 58.

(50) Rabow, L. E.; Stubbe, J.; Kozarich, J. W.; McGall, G. H. *J. Am. Chem. Soc.* **1990**, *112*, 3203.

(51) Povirk, L. F.; Wubker, W.; Koehnlein, W.; Hutchinson, F. *Nucleic Acids Res.* **1977**, *4*, 3573.

(52) Povirk, L. F.; Han, Y. H.; Steighner, R. J. *Biochemistry* **1989**, *28*, 5808.

(53) Stubbe, J.; Kozarich, J.W.; Wu, W.; Vanderwall, D. E. *Acc. Chem. Res.* **1996**, *29*, 322.

(54) Wu, W.; Vanderwall, D. E.; Stubbe, J.; Kozarich, J. W.; Turner, C. J. *J. Am. Chem. Soc.* **1994**, *116*, 10843.

(55) Wu, W.; Vanderwall, D. E.; Lui, S. M.; Tang, X.J.; Turner, C. J.; Kozarich, J. W.; Stubbe, J. *J. Am. Chem. Soc.* **1996**, *118*, 1268.

(56) Hoehn, S. T.; Junker, H.D.; Bunt, R. C.; Turner, C. J.; Stubbe, J. *Biochemistry* **2001**, *40*, 5894.

(57) Chen, J.; Stubbe, J. *Curr. Opin. Chem. Biol.* **2004**, *8*, 175.

(58) Keck, M. V.; Manderville, R. A.; Hecht, S. M. *J. Am. Chem. Soc.* **2001**, *123*, 8690.

(59) Akiyama, Y.; Ma, Q.; Edgar, E.; Laikhter, A.; Hecht, S. M. *J. Am. Chem. Soc.* **2008**, *130*, 9650.

(60) Ma, Q.; Akiyama, Y.; Xu, Z.; Konishi, K.; Hecht, S. M. *J. Am. Chem. Soc.* **2009**, *131*, 2013.

(61) Tan, J. D.; Farinas, E. T.; David, S. S.; Mascharak, P. K. *Inorg. Chem.* **1994**, *33*, 4295.

(62) Wu, W.; Vanderwall, D. E.; Turner, C. J.; Hoehn, S.; Chen, J.; Kozarich, J. W.; Stubbe, J. *Nucleic Acids Res.* **2002**, *30*, 4881.

(63) Manderville, R. A.; Ellena, J. F.; Hecht, S. M. *J. Am. Chem. Soc.* **1995**, *117*, 7891.

(64) McLean, M. J.; Dar, A.; Waring, M. J. *J. Mol. Recognit.* **1989**, *1*, 184.

(65) Akiyama, Y.; Ma, Q.; Edgar, E.; Laikhter, A.; Hecht, S. M. *Org. Lett.* **2008**, *10*, 2127.

(66) Absalon, M. J.; Wu, W.; Kozarich, J. W.; Stubbe, J. *Biochemistry* **1995**, *34*, 2076.

(67) Maxam, A. M.; Gilbert, W. *Methods Enzymol.* **1980**, *65*.

(68) Rubin, C. M.; Schmid, C. W. *Nucleic Acids Res.* **1980**, *8*, 4613.